individual wells in a volume of 20 μl, and the cells were incubated for 72 h at 37°C in humidified air containing 5% CO_2. MTT reagents (MTT, Sigma) were then added to each well in a volume of 20 μl, and the cells were incubated for 4 h at 37°C in humidified air containing 5% CO_2. Finally, the growth inhibitory effect of each drug was assessed spectrophotometrically.

Drug treatment, RNA isolation and microarray hybridization

To obtain reference profiles representing the drug-induced genomic response, the PC-14 cells were grown on plastic culture dishes until they reached 80% confluency; they were then treated with TZT-1027, D10, VDS, VCR, VBL, TXL and TXT for 6 h at the IC_{50} concentration of each drug determined by MTT assay for 72 h. Cell pellets of the eight samples, including an untreated control, were collected by centrifugation, and the total RNA from each sample was isolated using a single-step guanidium thiocyanate procedure (ISOGEN; Nippon gene).[40] Single-channel labeling ^{32}P nylon membrane-based cDNA microarrays containing 588 genes were used (Atlas® Human Cancer cDNA Expression Array; BD Biosciences Clontech, Palo Alto, CA, USA). Protocols on array printing, labeling and hybridization are available at the BD Biosciences Clontech web site (http://www.bdbiosciences.com/clontech/atlas/index.shtml) The hybridization intensities on X-ray films (Gel Bond®, FMC Bio Products Rockland, ME, USA) were scanned and quantified using a BAS-2000II scanner and Array Gauge software (Fuji Film, Tokyo).

Microarray data analysis

The intensity values of each gene were log-2-transformed and median-normalized using Excel software. The changes in gene expression induced by drug exposure were calculated for each spot by dividing the intensity of the drug exposure samples by that of the untreated samples. The multidimensional scaling analysis, based on a principle component analysis, was performed using SIMCA-P software v10.5 (Umetrics, Sweden). Three-dimensional rendering of the gene profiles was graphed in a manner such that samples with similar expression profiles would lie closer to each other than those with dissimilar profiles. The heat map, which showed the correlation coefficient between each drug reference profile, was performed by *R* (http://cran.r-project.org/).

Functional analysis of identified genes

To analyze the functions of the clustered genes, a gene ontology analysis was performed using the EASE bioinformatics software package (http://apps1.niaid. nih.gov/david/upload.asp).[41,42] This software package was used to rank functional clusters by statistical over-representation of individual genes in specific categories relative to all genes in the same category on the array. The functional clusters used by EASE were derived from the classification systems of Gene Ontology (GO). The *P*-value to rank categories of genes by over-representation was calculated using Jackknife-Fisher exact probabilities. The threshold for selecting categories was a *P*-value of less than 0.01 and a minimum gene count of more than two. *P*-values in gene ontology are not equal to biological significance but are helpful in focusing on the processes most likely to be associated with the biological phenomena associated with aging. We also conducted further online database searches to refine many specific GO annotations.

Real-time RT-PCR

Real-time RT-PCR was performed using a Smart Cycler system (Takara) and a SYBR Green PCR kit. The reaction solution was assembled in a volume of 25 μl comprised of TaqMan™ Universal PCR Master Mix (Applied Biosystems, Foster City, CA, USA), forward and reverse primers (final concentration, 0.2 μmol/l each) and cDNA mixture (≈2.5 ng) to produce PCR products specific for *GSTP1* and *TIMP3*. The primers and probes were purchased from Sigma-GenoSys (Tokyo, Japan). The conditions for real-time RT-PCR were preheating at 95°C for 10 min, followed by 40 cycles of shuttle heating at 95°C for 15 s and at 60°C for 20 s. A threshold was set in the linear part of the amplification curve, and the number of cycles needed to reach it was calculated for every gene. Relative mRNA levels were determined using the included standard curves for each individual gene and further normalized to the GAPDH mRNA level. Melting curves were used to establish the purity of the amplified band. The sequences of the primers used for RT-PCR were as follows: GSTO1 forward, 5′-AGG TTC TGC CCG TTT GCT GAG AGG and reverse, 5′-CAA GCT TTC TCA TAG GGG TCA TCC G; TIMP3 forward, 5′-TGC TGA CAG GTC GCG TCT ATG ATG G and reverse, 5′-GCG TAG TGT TTG GAC TGG TAG CCA G; GAPDH forward, 5′-TGA AGG TCG GAG TCA ACG GAT TTG GT and reverse, 5′-CAT GTG GGC CAT GAG GTC CAC CAC.

Acknowledgments

This study was supported in part by a Grant-in-Aid for Cancer Research and the 3rd Term Comprehensive 10-Year Strategy for Cancer Control from the Ministry of Health, Labour and Welfare, Tokyo, Japan. K Nishio and T Shimoyama designed the study. T Shimoyama and K Nishio prepared the manuscript. Y Koh and T Natsume undertook the study. T Shimoyama and T Hamano performed the statistical analysis. T Shimoyama is the recipient of a Research Resident Fellowship from the Foundation of Promotion of Cancer Research in Japan.

Duality of Interest

None declared.

References

1 Pettit G, Kamano Y, Herald C, Tuinman A, Boettner F, Kizu H *et al.* The isolation and structure of a remarkable marine animal antineoplastic constituent: dolastatin 10. *J Am Chem Soc* 1987; 109: 6883–6885.
2 Saad ED, Kraut EH, Hoff PM, Moore Jr DF, Jones D, Pazdur R *et al.* Phase II study of dolastatin-10 as first-line treatment for advanced colorectal cancer. *Am J Clin Oncol* 2002; 25: 451–453.

3 Vaishampayan U, Glode M, Du W, Kraft A, Hudes G, Wright J *et al.* Phase II study of dolastatin-10 in patients with hormone-refractory metastatic prostate adenocarcinoma. *Clin Cancer Res* 2000; **6**: 4205–4208.
4 Krug LM, Miller VA, Kalemkerian GP, Kraut MJ, Ng KK, Heelan RT *et al.* Phase II study of dolastatin-10 in patients with advanced non-small-cell lung cancer. *Ann Oncol* 2000; **11**: 227–228.
5 Margolin K, Longmate J, Synold TW, Gandara DR, Weber J, Gonzalez R *et al.* Dolastatin-10 in metastatic melanoma: a phase II and pharmokinetic trial of the California Cancer Consortium. *Invest New Drugs* 2001; **19**: 335–340.
6 Miyazaki K, Kobayashi M, Natsume T, Gondo M, Mikami T, Sakakibara K *et al.* Synthesis and antitumor activity of novel dolastatin 10 analogs. *Chem Pharm Bull (Tokyo)* 1995; **43**: 1706–1718.
7 Kobayashi M, Natsume T, Tamaoki S, Watanabe J, Asano H, Mikami T *et al.* Antitumor activity of TZT-1027, a novel dolastatin 10 derivative. *Jpn J Cancer Res* 1997; **88**: 316–327.
8 Chaplin DJ, Pettit GR, Parkins CS, Hill SA. Antivascular approaches to solid tumour therapy: evaluation of tubulin binding agents. *Br J Cancer Suppl* 1996; **27**: S86–S88.
9 Otani M, Natsume T, Watanabe JI, Kobayashi M, Murakoshi M, Mikami T *et al.* TZT-1027, an antimicrotubule agent, attacks tumor vasculature and induces tumor cell death. *Jpn J Cancer Res* 2000; **91**: 837–844.
10 Natsume T, Watanabe J, Koh Y, Fujio N, Ohe Y, Horiuchi T *et al.* Antitumor activity of TZT-1027 (Soblidotin) against vascular endothelial growth factor-secreting human lung cancer *in vivo*. *Cancer Sci* 2003; **94**: 826–833.
11 Niitani H, Hasegawa K. Phase I studies of TZT-1027, a novel inhibitor of tubulin polymerization. *Ann Oncol* 1998; **9**(Suppl 2): 360.
12 de Jonge MJ, van der Gaast A, Planting AS, van Doorn L, Lems A, Boot I *et al.* Phase I and pharmacokinetic study of the dolastatin 10 analogue TZT-1027, given on days 1 and 8 of a 3-week cycle in patients with advanced solid tumors. *Clin Cancer Res* 2005; **11**: 3806–3813.
13 Schoffski P, Thate B, Beutel G, Bolte O, Otto D, Hofmann M *et al.* Phase I and pharmacokinetic study of TZT-1027, a novel synthetic dolastatin 10 derivative, administered as a 1-hour intravenous infusion every 3 weeks in patients with advanced refractory cancer. *Ann Oncol* 2004; **15**: 671–679.
14 Natsume T, Watanabe J, Tamaoki S, Fujio N, Miyasaka K, Kobayashi M. Characterization of the interaction of TZT-1027, a potent antitumor agent, with tubulin. *Jpn J Cancer Res* 2000; **91**: 737–747.
15 Fujita F, Koike M, Fujita M, Sakamoto Y, Tsukagoshi S. Antitumor effects of TZT-1027, a novel dolastatin 10 derivative, on human tumor xenografts in nude mice. *Gan To Kagaku Ryoho* 2000; **27**: 451–458.
16 Watanabe J, Natsume T, Fujio N, Miyasaka K, Kobayashi M. Induction of apoptosis in human cancer cells by TZT-1027, an antimicrotubule agent. *Apoptosis* 2000; **5**: 345–353.
17 Natsume T, Kobayashi M, Fujimoto S. Association of p53 gene mutations with sensitivity to TZT-1027 in patients with clinical lung and renal carcinoma. *Cancer* 2001; **92**: 386–394.
18 Natsume T, Nakamura T, Koh Y, Kobayashi M, Saijo N, Nishio K. Gene expression profiling of exposure to TZT-1027, a novel microtubule-interfering agent, in non-small cell lung cancer PC-14 cells and astrocytes. *Invest New Drugs* 2001; **19**: 293–302.
19 DeRisi JL, Iyer VR, Brown PO. Exploring the metabolic and genetic control of gene expression on a genomic scale. *Science* 1997; **278**: 680–686.
20 Parsons AB, Brost RL, Ding H, Li Z, Zhang C, Sheikh B *et al.* Integration of chemical-genetic and genetic interaction data links bioactive compounds to cellular target pathways. *Nat Biotechnol* 2004; **22**: 62–69.
21 Baetz K, McHardy L, Gable K, Tarling T, Reberioux D, Bryan J *et al.* Yeast genome-wide drug-induced haploinsufficiency screen to determine drug mode of action. *Proc Natl Acad Sci USA* 2004; **101**: 4525–4530.
22 Kung C, Kenski DM, Dickerson SH, Howson RW, Kuyper LF, Madhani HD *et al.* Chemical genomic profiling to identify intracellular targets of a multiplex kinase inhibitor. *Proc Natl Acad Sci USA* 2005; **102**: 3587–3592.
23 Gunther EC, Stone DJ, Gerwien RW, Bento P, Heyes MP. Prediction of clinical drug efficacy by classification of drug-induced genomic expression profiles *in vitro*. *Proc Natl Acad Sci USA* 2003; **100**: 9608–9613.
24 DeVita VT, Hellman S, Rosenberg SA. *Cancer: Principles and Practice of Oncology*, 7th edn, Lippincott Williams & Wilkins (LWW): Philadelphia, 2004.
25 Jordan MA, Wilson L. Microtubules as a target for anticancer drugs. *Nat Rev Cancer* 2004; **4**: 253–265.
26 Diaz JF, Andreu JM. Assembly of purified GDP-tubulin into microtubules induced by taxol and taxotere: reversibility, ligand stoichiometry, and competition. *Biochemistry* 1993; **32**: 2747–2755.
27 Jordan A, Hadfield JA, Lawrence NJ, McGown AT. Tubulin as a target for anticancer drugs: agents which interact with the mitotic spindle. *Med Res Rev* 1998; **18**: 259–296.
28 Gupta S, Bhattacharyya B. Antimicrotubular drugs binding to *Vinca*domain of tubulin. *Mol Cell Biochem* 2003; **253**: 41–47.
29 Bai RL, Paull KD, Herald CL, Malspeis L, Pettit GR, Hamel E. Halichondrin B and homohalichondrin B, marine natural products binding in the *Vinca*domain of tubulin. Discovery of tubulin-based mechanism of action by analysis of differential cytotoxicity data. *J Biol Chem* 1991; **266**: 15882–15889.
30 Etienne-Manneville S, Hall A. Rho GTPases in cell biology. *Nature* 2002; **420**: 629–635.
31 Sahai E, Marshall CJ. RHO-GTPases and cancer. *Nat Rev Cancer* 2002; **2**: 133–142.
32 Board PG, Coggan M, Chelvanayagam G, Easteal S, Jermiin LS, Schulte GK *et al.* Identification, characterization, and crystal structure of the Omega class glutathione transferases. *J Biol Chem* 2000; **275**: 24798–24806.
33 Schisselbauer JC, Silber R, Papadopoulos E, Abrams K, LaCreta FP, Tew KD. Characterization of glutathione S-transferase expression in lymphocytes from chronic lymphocytic leukemia patients. *Cancer Res* 1990; **50**: 3562–3568.
34 Ban N, Takahashi Y, Takayama T, Kura T, Katahira T, Sakamaki S *et al.* Transfection of glutathione S-transferase (GST)-pi antisense complementary DNA increases the sensitivity of a colon cancer cell line to adriamycin, cisplatin, melphalan, and etoposide. *Cancer Res* 1996; **56**: 3577–3582.
35 Anand-Apte B, Bao L, Smith R, Iwata K, Olsen BR, Zetter B *et al.* A review of tissue inhibitor of metalloproteinases-3 (TIMP-3) and experimental analysis of its effect on primary tumor growth. *Biochem Cell Biol* 1996; **74**: 853–862.
36 Hiraoka N, Allen E, Apel IJ, Gyetko MR, Weiss SJ. Matrix metalloproteinases regulate neovascularization by acting as pericellular fibrinolysins. *Cell* 1998; **95**: 365–377.
37 Anand-Apte B, Pepper MS, Voest E, Montesano R, Olsen B, Murphy G *et al.* Inhibition of angiogenesis by tissue inhibitor of metalloproteinase-3. *Invest Ophthalmol Vis Sci* 1997; **38**: 817–823.
38 Qi JH, Ebrahem Q, Moore N, Murphy G, Claesson-Welsh L, Bond M *et al.* A novel function for tissue inhibitor of metalloproteinases-3 (TIMP3): inhibition of angiogenesis by blockage of VEGF binding to VEGF receptor-2. *Nat Med* 2003; **9**: 407–415.
39 Mosmann T. Rapid colorimetric assay for cellular growth and survival: application to proliferation and cytotoxicity assays. *J Immunol Methods* 1983; **65**: 55–63.
40 Chomczynski P, Sacchi N. Single-step method of RNA isolation by acid guanidinium thiocyanate-phenol-chloroform extraction. *Anal Biochem* 1987; **162**: 156–159.
41 Hosack DA, Dennis Jr G, Sherman BT, Lane HC, Lempicki RA. Identifying biological themes within lists of genes with EASE. *Genome Biol* 2003; **4**: R70.
42 Dennis Jr G, Sherman BT, Hosack DA, Yang J, Gao W, Lane HC *et al.* DAVID: database for annotation, visualization, and integrated discovery. *Genome Biol* 2003; **4**: P3.

Supplementary Information accompanies the paper on The Pharmacogenomics Journal website (http://www.nature.com/tpj).

Int. J. Cancer: **118**, 483–489 (2006)

ZD6474 inhibits tumor growth and intraperitoneal dissemination in a highly metastatic orthotopic gastric cancer model

Tokuzo Arao[1,2,4], Kazuyoshi Yanagihara[3], Misato Takigahira[3], Masayuki Takeda[1,2], Fumiaki Koizumi[1,2], Yasushi Shiratori[4] and Kazuto Nishio[1,2]*

[1]*Shien Lab, Medical Oncology, National Cancer Center Hospital, Tokyo, Japan*
[2]*Pharmacology Division, National Cancer Center Research Institute, Tokyo, Japan*
[3]*Central Animal Laboratory, National Cancer Center Research Institute, Tokyo, Japan*
[4]*Department of Gastroenterology and Hepatology, Okayama University Graduate School of Medicine and Dentistry, Okayama, Japan*

Angiogenesis inhibitors have been used to treat some cancers, but the therapeutic potential of these agents for gastric cancer has remained unclear. To investigate their therapeutic potential, we examined the effect of ZD6474, an agent that selectively targets vascular endothelial growth factor receptor-2 (VEGFR-2; KDR) tyrosine kinase and epidermal growth factor receptor (EGFR) tyrosine kinase, in a highly metastatic orthotopic model using an undifferentiated gastric cancer cell line, 58As1. ZD6474 (100 mg/kg/day, p.o., 2 weeks) significantly inhibited tumor growth ($p < 0.05$ *vs.* control) and reduced tumor dissemination into the peritoneal cavity ($p < 0.05$ *vs.* control). In addition, to identify putative tumor biomarkers that would reflect the effects of ZD6474 treatment in clinical settings, we examined the gene expression profiles of implanted gastric tumors treated with ZD6474 *in vivo*. Twenty-eight candidate genes were identified, including *IGFBP-3*, *ADM*, *ANGPTL4*, *PLOD2*, *DSIPI*, *NDRG1*, *ENO2*, *HIG2* and *BNIP3L*, which are known to be hypoxia-inducible genes. These genes and gene products may be useful biomarkers for monitoring the effects of ZD6474 treatment. ZD6474 also improved the survival of mice with implanted another undifferentiated gastric cancer cell line, 44As3. In conclusion, our results suggest that ZD6474 may have clinical activity against gastric cancer, particularly undifferentiated gastric cancer with peritoneal dissemination. We also identified putative biomarkers for monitoring the pharmacodynamic effects of ZD6474 by gene expression profiling.
© *2005 Wiley-Liss, Inc.*

Key words: ZD6474; gastric cancer; intraperitoneal dissemination; VEGF; oligonucleotide microarray

Various anti-cancer agents have been examined for efficacy against gastric cancer over the past two decades, but the median survival time of patients remains around 7 months,[1,2] and the prognosis of gastric cancer patients remains poor. Peritoneal dissemination is common in patients with unresectable gastrointestinal cancer, and many suffer from peritoneal carcinomatosis in the terminal stage. Because undifferentiated gastric cancer is particularly invasive and often accompanied by peritoneal dissemination,[3] a new treatment strategy is needed.

Vascular endothelial growth factor (VEGF) is a key mediator of tumor growth and is known to have multiple functions in angiogenesis, vascular permeability, and the regulation of endothelial cell proliferation and migration.[1–6] VEGF receptors (VEGFR) are activated by ligand stimulation with VEGF and commonly expressed in vascular endothelial cells. VEGFR-2 (KDR/Flk-1) is thought to be important for angiogenesis.[7] Because the VEGF-VEGFR system plays a key role in angiogenesis and tumor growth *in vivo*, the therapeutic potential of many agents targeting this system is being investigated.[8] A recent study has shown that a combination of monoclonal antibody against VEGF and chemotherapy produces a clinically meaningful survival benefit for patients with metastatic colorectal cancer,[5] and these results may lead to changes in the standard treatment for colorectal cancer.[9]

ZD6474 is a novel orally available VEGFR-2 (KDR) tyrosine kinase inhibitor that is also known to selectively target epidermal growth factor receptor (EGFR) tyrosine kinase, both of which are parts of key pathways in tumor growth.[10–13] We demonstrated previously the evidence suggesting that ZD6474 inhibits angiogenesis and tumor growth by targeting EGFR.[14,15]

In our present study, we tested ZD6474 for an inhibitory effect on tumor growth and intraperitoneal dissemination, and for improvement of survival in a newly established, highly metastatic orthotopic gastric tumor model *in vivo*. In addition, we also identified putative biomarkers to monitor the effects of ZD6474 treatment using gene expression profiling.

Material and methods

Reagents

ZD6474 and gefitinib (Iressa®) were provided by AstraZeneca (Cheshire, UK).

Cell cultures

The newly established highly metastatic human signet-ring cell gastric cancer cell lines 58As1 and 44As3 produce large volumes of ascitic fluid and spontaneously metastasize to the peritoneal cavity after orthotopic (gastric wall) implantation.[16,17] 58As1 and 44As3 and human non-small cell lung cancer cell line PC-9 were maintained in RPMI-1640 medium (Sigma, St. Louis, MO) supplemented with 10% heat-inactivated FBS (Gibco BRL, Grand Island, NY). The PC-9 cells were a gift of Tokyo Medical University. Human embryonic kidney cell line 293 (HEK293) was obtained from the American Type Culture Collection (Manassas, VA) and cultured in DMEM supplemented with 10% FBS. Human umbilical vein endothelial cells (HUVEC) were maintained in EBM-2 medium (Clonetics, Walkersville, MD) supplemented with EGM-2 kit (Clonetics), according to the manufacturer's instructions.

In vitro *growth-inhibition assay*

The cell-growth inhibitory effects of ZD6474 and gefitinib were assessed by the thiazole blue tetrazolium bromide (MTT) assay (Sigma). Briefly, 180 μl/well of cell suspension was seeded on to Sumilon® 96-well microculture plates (Sumitomo Bakelite, Akita, Japan) and incubated in 10% FBS-containing medium for 24 hr. The cells were then treated with ZD6474 at various concentrations (4 nM–80 μM) and cultured at 37°C in a humidified atmosphere for 72 hr. After the culture period, 20 μl volume of MTT reagent was added, and the plates were further incubated for 4 hr. After centrifuging the plates, the culture medium was discarded and the wells were filled with dimethyl-sulfoxide. The optical density of the cultures was measured at 562 nm with Delta-soft software on a

Grant sponsor: Ministry of Education, Culture, Sports, Science and Technology of Japan; Grant number: 12217165
*Correspondence to: Shien Lab, Medical Oncology, National Cancer Center Hospital, Tsukiji 5-1-1, Chuo-ku, Tokyo 104-0045, Japan.
Fax: +81-3-3547-5185. E-mail: knishio@gan2.res.ncc.go.jp
Received 14 March 2005; Accepted after revision 18 May 2005
DOI 10.1002/ijc.21340
Published online 28 July 2005 in Wiley InterScience (www.interscience.wiley.com).

Macintosh computer interfaced to a Bio-Tek Microplate Reader EL-340 (BioMetallics, Princeton, NJ). The experiment was conducted in triplicate.

Immunoblotting

EGFR, phospho-EGFR (specific for Tyr 1068), and anti-rabbit horseradish peroxidase (HRP)-conjugated antibody were purchased from Cell Signalling (Beverly, MA). Cell pellets were lysed in RIPA buffer (Tris-HCl, 50 mM; pH 7.4; NP-40, 1%; Na-deoxycholate, 0.25%; NaCl, 150 mM; EDTA, 1 mM; phenylmethyl-sulfonyl fluoride, 1 mM; aprotinin, leupeptin, pepstatin, 1 mg/ml each; Na_3VO_4, 1 mM; NaF, 1 mM). Cell extracts were electrophoresed on 7.5% (w/v) polyacrylamide gels and transferred to a polyvinylidene di-fluoride membrane (Nihon Millipore, Tokyo, Japan). The membrane was incubated in Tris-buffered saline containing 0.5% Tween 20 with 3% BSA and then reacted with the primary antibodies and the HRP-conjugated secondary antibody for 90 min each. Visualization was achieved with an enhanced chemiluminescent detection reagent (Amersham Bioscience, Buckinghamshire, UK).

RT-PCR

A 5 μg of total RNA from each cultured cell line was converted to cDNA with a GeneAmp® RNA-PCR kit (Applied Biosystems, Foster City, CA). The primers used for the PCR were: human-specific beta-actin, forward: 5′-GGAAATCGTGCGTGACATT-3′ and reverse: 5′-CATCTGCTGGAAGGTGGACAG-3′; mouse-specific beta-actin, forward: 5′-GAAATCGTGCGTGACATCAAA-3′ and reverse: 5′-TCATGGTGCTAGGAGCCA-3′; VEGF-A, forward: 5′-GCCTTG-CCTTGCTGCTCTAC-3′ and reverse: 5′-CA-GGGATTTTCTTGTC-TTGC-3′; VEGF-C, forward: 5′-AAACAAGGAGCTGGATGAA-GAG-3′ and reverse: 5′-CAATATGAAGGGACACAACGAC-3′; VEGFR-1, forward: 5′-TAGCGTCACCAGCAGCGAAAGC-3′ and reverse: 5′-CCTTTCTTTTGGGTCTCTGTGC-3′; VEGFR-2, forward: 5′-CAGACGGAC-AGTGGTATGGTTC-3′ and reverse: 5′-ACCTGCTGGTGGAAAGAACAAC-3′; VEGFR-3, forward: 5′-AGCCATTCATCAACAAGCCT-3′ and reverse: 5′-GGCAACAG-CTGGATGTCATA-3′; IGFBP3, forward: 5′- AATGCTAGTGA-GTCGGAGGAAGAC-3′ and reverse: 5′- GGCGACACTGCTTTT-TCTTATAAA-3′; ADM, forward: 5′- CCTGGGTTCGCTCGCCTT-CCTA-3′ and reverse: 5′- GGCTGGAGCCCCGTGTG- CTTGT-3′.

PCR amplification was carried out for 35 cycles (95°C for 45 sec, 56–62°C for 45 sec, and 72°C for 60 sec) with a final extension step at 72°C for 7 min. The bands were visualized by ethidium bromide staining.

Sequencing

Exons 18–21 of the EGFR cDNA from the tumor cell lines were sequenced, and the cDNAs were amplified using the following primers: forward, 5′-TCCAAACTGCACCTACGGATGC-3′, and reverse, 5′-CATCAACTCCCAAACGGTCACC-3′. The PCR amplification consisted of 25 cycles (95°C for 45 sec, 55°C for 30 sec and 72°C for 60 sec). The sequences of the PCR products were determined using ABI prism 310 (Applied Biosystems). Amplification and sequencing were carried out in duplicate for each tumor cell line. The sequences were compared to the GenBank-archived human sequence of EGFR (accession number: NM_005228.3).

Orthotopic model in vivo

ZD6474 was dissolved in sterile water containing 1% TWEEN 80 (Sigma). Six-week old female BALB/c nude mice were purchased from CLEA Japan Inc. (Tokyo) and maintained under specific pathogen-free conditions. A total of 1×10^6 58As1 cells was inoculated into the gastric wall of each mouse after laparotomy. Three days after the inoculation, the mice were given ZD6474 50 mg/kg/day (n = 6) or 100 mg/kg/day (n = 6) or a vehicle control (n = 6) p.o. for 14 days. After euthanizing the mice on Day 19, tumor volume was measured and tumor samples and intraperitoneal lavage fluid were collected. The tumor samples were formalin fixed (n = 3) or stored in Isogen (n = 3) (Nippon Gene, Tokyo, Japan). The intraperitoneally disseminated cells were collected from 2 ml of PBS that had been used to wash the peritoneal cavity.

In the survival study, mice were inoculated with 1×10^6 58As1 or 44As3 cells into the gastric wall after laparotomy. Three days after inoculation, the mice were given ZD6474 50 mg/kg/day of ZD6474 p.o. (n = 7) or i.p. (n = 7) or the vehicle control p.o. (n = 7) for 14 days. The "visible ascites," which was evident a few days before death in this model, was used as a surrogate for survival time to consider for animal welfare. Mice were euthanized when ascites became visible, implantation of the gastric cancer cells was confirmed in all of the euthanized mice. No cancer cell was found in one mouse (ZD6474 100 mg/kg/day, 44As3 implanted), and it was excluded from the analysis. The experimental animal protocols were approved by the Committee for Ethics of Animal Experimentation, and the experiments were conducted in accordance with the Guidelines for Animal Experiments of the National Cancer Center.

Oligonucleotide microarray study

A DNA microarray procedure was used to prepare the *in vitro* transcription products, and oligonucleotide array hybridization and scanning were carried out according to the Affymetrix protocols (Santa Clara, CA). In brief, total RNA extracted from the tumor samples was analyzed with the Agilent 2100 Bioanalyzer (Agilent Technologies, Waldbronn, Germany) and cRNA was synthesized with the GeneChip® 3′-Amplification Reagents One-Cycle cDNA Synthesis Kit (Affymetrix). The cRNA were then labeled and purified for use as probes. Hybridization was carried out to the Affymetrix GeneChip HG-U133 Plus2.0 array for 16 hr at 45°C. After washing the glass slides, spot intensity was measured by scanning with a GeneChip® Scanner3000 (Affymetrix) and converted to numerical data with GeneChip Operating Software, Ver.1 (Affymetrix).

Six GeneChips were used to primary implanted 58as1 tumor samples from the vehicle control group (n = 2), and the ZD6474-treated group (n = 2, 50 mg/kg group; n = 2, the 100 mg/kg group).

Statistical analysis

All statistical calculations, except the analysis of the microarray data, were carried out using StatView version 5 software (SAS Institute Inc., Cary, NC). A p-value of <0.05 was considered significant. The microarray data were analyzed with GeneSpring software (Silicon Genetics, Redwood City, CA). The expression data were normalized across the sample set by the 50th percentile of each chip's intensity range. Relative expression data for each probe set were generated by median normalization. The fold change (mean value of the ZD6474-treatment group/mean value of the vehicle control group) was calculated, and genes with >2-fold change or <0.5-fold change were selected.

Results

Cell sensitivity to ZD6474 in vitro and expression of EGFR and EGFR

Cell sensitivity to ZD6474 and the expression levels of EGFR, VEGFR and VEGF were examined in the 58As1 cells. The growth-inhibitory effect of ZD6474 and gefitinib was assessed by an MTT assay. The IC_{50} values of ZD6474 and gefitinib for 58As1 cells were 5.8 ± 1.8 and 11.0 ± 3.0 μM, respectively, suggesting that 58As1 cells are not sensitive to ZD6474 or gefitinib *in vitro*, compared to the "hypersensitive" PC-9 cells (IC_{50} values 0.09 and 0.03 μM, respectively).[15] The 58As1 cells expressed a relatively high level of EGFR compared to the cells expressing high (PC-9) and low (HEK293) levels of EGFR, but the phosphorylation status was low (Fig. 1*a*). The expression levels of VEGFR and VEGF-A/C were measured by RT-PCR. A low

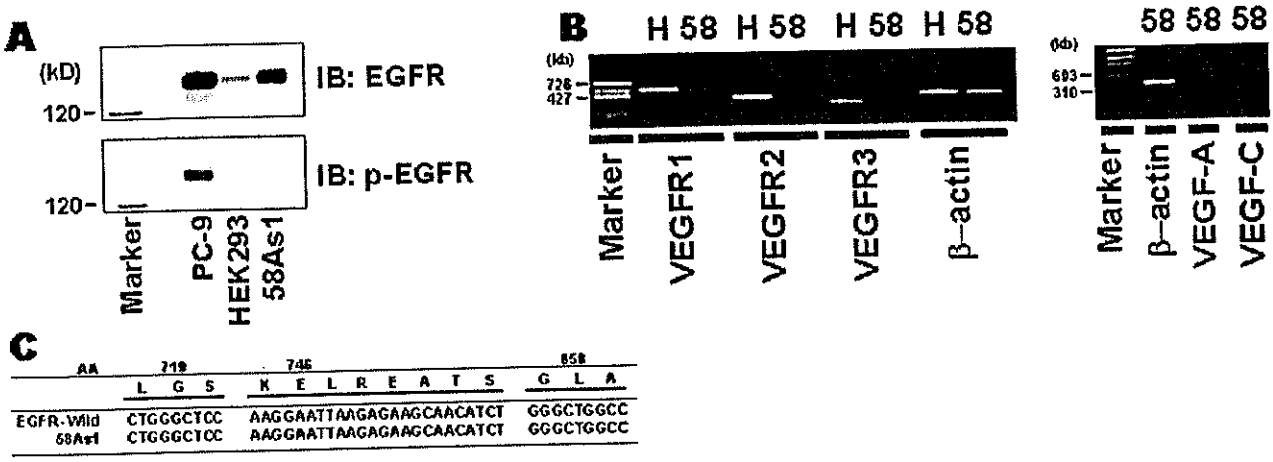

FIGURE 1 -- Cellular characteristics of 58As1 cells. (*a*) EGFR expression and phosphorylation levels determined by Western blotting. A moderately high level of EGFR expression was observed in 58As1 cells, compared to cells expressing high (PC-9) and low (HEK293) levels of EGFR. The phosphorylation of EGFR status in 58As1 cells was low under normal culture conditions. IB, immunoblotting. Molecular marker: 120 kD. (*b*) Expression levels of VEGFR and VEGF-A and VEGF-C were measured by RT-PCR. A low level of VEGFR1 expression was detected in 58As1 cells, but no expression of VEGFR-2 or 3 was detected. 58As1 cells expressed VEGF-A but not VEGF-C. H, human umbilical vein endothelial cells. 58: 58As1. (*c*) EGFR sequence in 58As1 cells. No mutations were detected near the ATP-binding domains in 58As1 cells. AA, amino acid.

level of VEGFR1 expression was found in the 58As1 cells, but no VEGFR2 or VEGFR3 expression was detected. The 58As1 cells expressed VEGF-A, but not VEGF-C (Fig. 1*b*). Our results suggest that the lymphatic-metastasis-related VEGF-C and VEGFR3 are not involved in the inhibitory effect of ZD6474 on tumor dissemination observed in our present study *in vivo*.

Because EGFR mutations may be a determinant of tumor cell sensitivity to ZD6474,[15] exons 18–21 of EGFR mRNA from 58As1 cells were sequenced. No mutations near the ATP-binding domains[18,19] were detected, the 58As1 cells were concluded to express the wild-type EGFR.

Growth-inhibitory effect of ZD6474 in the orthotopic model in vivo

To examine the antitumor effect of ZD6474 on gastric cancer, we assessed the growth-inhibitory effect of ZD6474 by measuring implanted tumor volume after 14 days of p.o. treatment *in vivo*. A significant growth-inhibitory effect was observed in the ZD6474 (100 mg/kg/day) group in comparison with the vehicle control group ($p = 0.027$) in athymic mice implanted with 58As1 cells (Fig. 2*a*). Average tumor volume in the vehicle control group, 50 mg/kg/day ZD6474 group and 100 mg/kg/day ZD6474 groups was 106.3 ± 81.8 mm^3, 79.9 ± 70.0 mm^3, and 42.3 ± 24.8 mm^3, respectively.

Histological examination of H&E stained specimens showed a marked reduction in the number of cancer cells in the sub-mucosal lesions and the presence of necrotic tissue in the ZD6474 groups (Fig. 2*b*), suggesting that ZD6474 inhibits the growth of primary gastric tumor *in vivo*.

Inhibitory-effect of ZD6474 on peritoneal dissemination

To monitor the inhibitory effect of ZD6474 on peritoneally disseminated human cancer cells, the mRNA expression ratio of human β-actin/murine β-actin was measured with appropriate specific primers in cells collected from intraperitoneal lavage fluid. A significantly lower level of human-derived β-actin was observed in the 100 mg/kg/day ZD6474 group than in the vehicle control group ($p = 0.049$) (Fig. 2*c*,*d*), indicating that ZD6474 inhibits the intraperitoneal dissemination of gastric cancer in a dose-dependent manner.

Effect of ZD6474 on survival

In the survival experiment, we examined the effect of ZD6474 (p.o. or i.p.) on the survival of mice implanted with 58As1 or 44As3 cells. Both p.o. and i.p. administration of ZD6474 50 mg/kg/day significantly improved the survival of 44As3-implanted mice ($p = 0.0009$, $p = 0004$ *vs.* control, Fig. 3*b*), but did not significantly improve the survival of 58As1-implanted mice ($p = 0.09$, $p = 0.4$ *vs.* control, Fig. 3*a*). The median survival time of the 58As1-implanted mice was 33 days in the control group, 40 days in the i.p. group, and 46 days in the *p.o.* group, whereas in the 44As3-implanted mice, it was 34 days, 43 days and 53 days, respectively. Oral administration of ZD6474 was more effective than i.p. injection ($p = 0.049$) in the 44As3-implanted mice (Fig. 3*b*). These results suggest that ZD6474 is an active against gastric cancer.

Regulation of the gene expression by ZD6474 in vivo

To identify putative tumor biomarkers that reflect the efficacy of ZD6474 in vivo, we analyzed the gene expression profiles of implanted-tumor samples with oligonucleotide microarray. Expression of 26 genes was upregulated by 2-fold or more in the ZD6474 treatment group compared to the control group, whereas 2 genes were downregulated (Fig. 4*a*). Interestingly, of 26 upregulated genes, 9 of these genes were reported previously to be hypoxia-inducible: *IGFBP3* (*insulin-like growth factor binding protein 3*), *ADM* (*adrenomedullin*), *ANGPTL4* (*angiopoietin-like 4*), *PLOD2* (*procollagen-lysine, 2-oxoglutarate 5-dioxygenase 2*), *DSIPI* (*delta sleep inducing peptide, immunoreactor*), *ENO2* (*enolase 2*), *NDRG1* (*N-myc downstream regulated gene 1*) *HIG2 (hypoxia-inducible protein 2*) and *BNIP3L* (*BCL2/adenovirus E1B 19 kDa interacting protein 3-like*). To confirm upregulation of the genes, we measured the expression levels of representative genes, *IGFBP3* and *ADM*, by RT-PCR in murine tumor samples (Fig. 4*b*).

Discussion

A correlation between somatic EGFR mutations in non-small cell lung cancer cells and sensitivity to EGFR-specific tyrosine kinase inhibitors, including gefitinib and erlotinib, has been demonstrated recently,[18,20] and a similar observation was made in regard to ZD6474 *in vitro*.[15] We demonstrated previously that cells transfected with mutated EGFR were ~60-fold more sensitive to ZD6474 *in vitro*. EGFR tyrosine kinase inhibitors may pro-

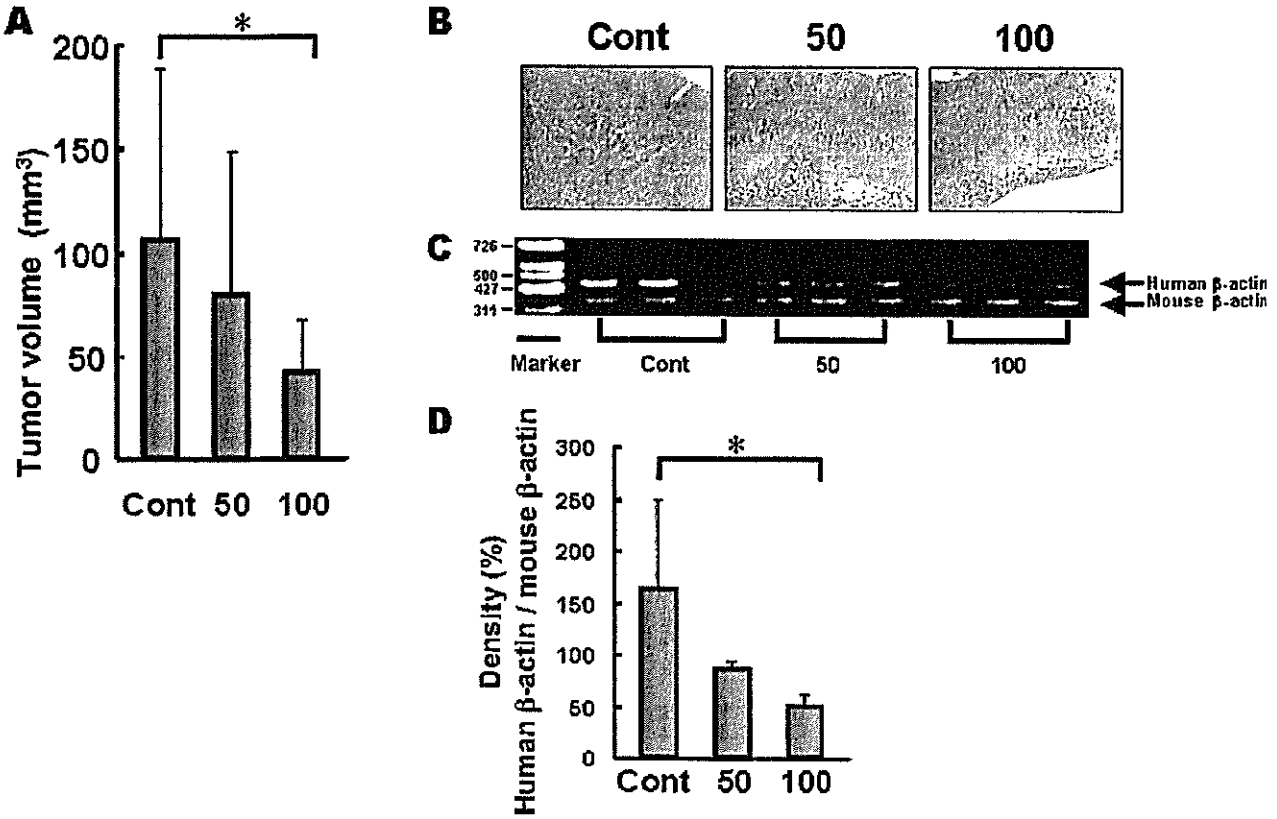

FIGURE 2 – Antitumor effect of ZD6474 in an orthotopic dissemination model *in vivo*. (*a*) *In vivo* growth-inhibitory effect of ZD6474. The implanted tumor volume was calculated after 14 days of treatment (p.o.). *Athymic mice ($n = 7$) per group were implanted with 58As1 cells, and a significant growth inhibitory effect was observed in the 100 mg/kg/day group, compared to the vehicle control group ($p = 0.027$). (*b*) Representative HE staining of tumor tissue in mice treated with ZD6474. The number of cancer cells in the sub-mucosal lesions was clearly lower and necrotic tissue was visible in the ZD6474 group, compared to the control group. (*c*) Disseminated cancer cells were collected from intraperitoneal lavage fluid to measure the ratio of tumor-derived human β-actin to murine β-actin using RT-PCR and specific primers (3 mice/group). Total RNA was equalized to 5 μg for each sample. (*d*) Densitometric analysis. Ratio of β-actin levels. *Significantly lower level of human-derived β-actin was detected in the 100 mg/kg/day ZD6474 group than in the control group ($p = 0.049$). The data shown are means ± SD. Cont, vehicle control; 50, ZD6474 50 mg/kg/day group; 100, ZD6474 100 mg/kg/day group. Significance was analyzed by Student's *t*-test.

vide particularly effective therapy for the subset of lung cancer patients whose tumor cell growth is highly dependent on EGFR signaling, including patients with tumor cells harboring activated, mutated EGFR. The proportion of patients with tumors highly dependent on EGFR signaling may be relatively small among various cancer patient populations. Therefore, additional treatment options for patients with cancers less dependent on EGFR signaling are also needed. It was concluded that 58As1 cells expressing wild-type EGFR are not highly dependent on EGFR signaling *in vitro* because the IC_{50} for growth inhibition by ZD6474 (5.8 μM) fell within the range of sensitivity reported by others for tumor cells *in vitro* (2.7–13.5 μM)[10] and because the IC_{50} for growth inhibition by gefitinib, a highly selective EGFR tyrosine kinase inhibitor, was >10μM. As a result, the concentration of ZD6474 required to inhibit 58As1 cell growth *in vitro* was 97-fold greater than required to inhibit VEGF-dependent HUVEC proliferation.[10] Nonetheless, ZD6474 significantly inhibited 58As1 tumor growth *in vivo* (Fig. 2*a*), suggesting that ZD6474 is active against gastric cancers expressing wild-type EGFR *in vivo* and that ZD6474 inhibition of tumor angiogenesis is likely to contribute significantly to this antitumor effect.

Our present study is unique because our aggressive and spontaneous intraperitoneal-dissemination model is considered a very good model of tumor progression in gastric cancer patients clinically, especially of the undifferentiated type. Indeed, Paclitaxel and CPT-11 have been demonstrated to exhibit a growth-inhibitory effect and survival benefit in this model,[17] but gefitinib did not in preliminary result (data not shown). The positive results with ZD6474 in our present study suggest that this agent may be clinically useful in gastric cancer. We had hypothesized that direct intraperitoneal injection of ZD6474 is more effective than oral administration to inhibit intraperitoneal dissemination and result in better survival, however, the result showed that oral administration led to better survival in 44As3-inplanted mice (Fig. 3*b*).

ZD6474 inhibited the intraperitoneal dissemination of gastric cancer cells in our dissemination model. Although the mechanisms underlying this effect remain unclear, a few possibilities can be speculated: based on clinical evidence, the depth of tumor invasion and clinical staging is thought to be closely related to peritoneal dissemination.[21] Thus, one possible mechanism of the reduction of intraperitoneal dissemination may have resulted from a reduction in the serosal penetration of the cancer cells by "antitumor effect of ZD6474" on the implanted tumors. Although it is unclear whether ZD6474 has an inhibitory effect against distal metastasis to the liver and lymph nodes, for examples, it is not surprising that ZD6474 inhibits "intraperitoneal dissemination." Evaluation of its effect on distal metastasis will be the subject of a future investigation in our laboratory. Small tumor lesions (up to 2 mm) may obtain the oxygen and nutrients

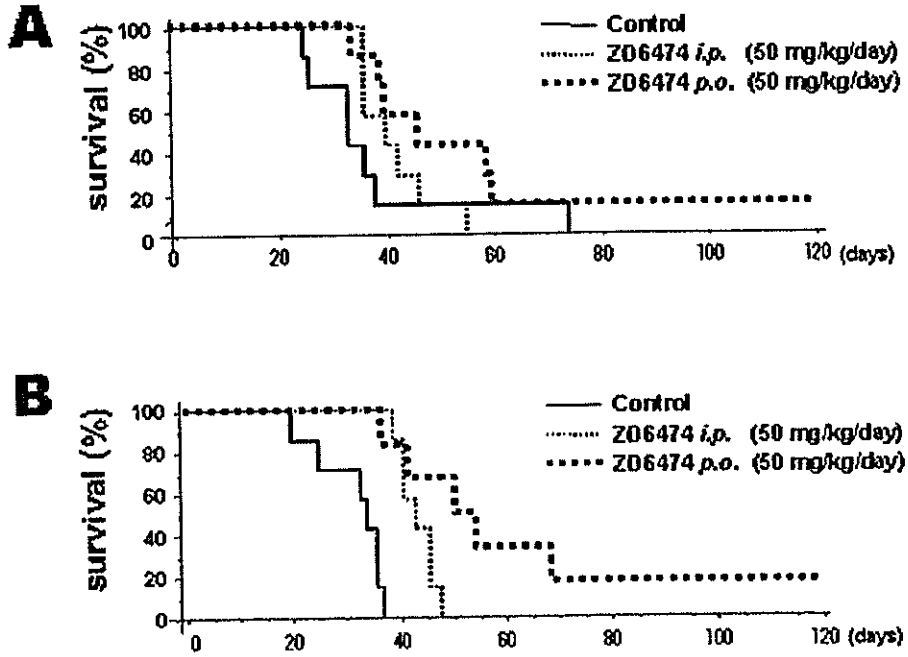

FIGURE 3 - Survival curve of 58As1 cells- (*a*) and 44As3 cells- (*b*) implanted mice treated with ZD6474. Both p.o. and i.p. administration of ZD6474 50 mg/kg/day significantly improved the survival of 44As3-implanted mice ($p = 0.0009$, $p = 0004$ *vs.* control), but did not significantly improve the survival of mice implanted with 58As1 cells ($p = 0.09$, $p = 0.4$ *vs.* control). The p values were calculated by the log-rank test.

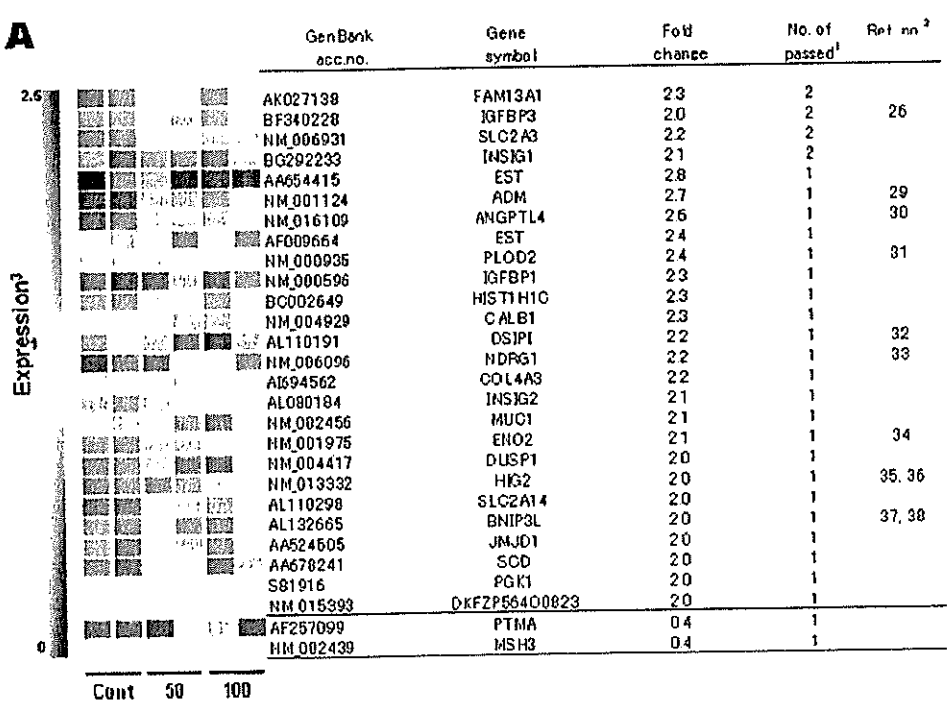

GenBank acc.no.	Gene symbol	Fold change	No. of passed[1]	Ref. no.[2]
AK027138	FAM13A1	2.3	2	
BF340228	IGFBP3	2.0	2	26
NM_006931	SLC2A3	2.2	2	
BG292233	INSIG1	2.1	2	
AA654415	EST	2.8	1	
NM_001124	ADM	2.7	1	29
NM_016109	ANGPTL4	2.6	1	30
AF009664	EST	2.4	1	
NM_000935	PLOD2	2.4	1	31
NM_000596	IGFBP1	2.3	1	
BC002649	HIST1H1C	2.3	1	
NM_004929	CALB1	2.3	1	
AL110191	DSIPI	2.2	1	32
NM_006096	NDRG1	2.2	1	33
AI694562	COL4A3	2.2	1	
AL080184	INSIG2	2.1	1	
NM_002456	MUC1	2.1	1	
NM_001975	ENO2	2.1	1	34
NM_004417	DUSP1	2.0	1	
NM_013332	HIG2	2.0	1	35, 36
AL110298	SLC2A14	2.0	1	
AL132665	BNIP3L	2.0	1	37, 38
AA524505	JMJD1	2.0	1	
AA676241	SCD	2.0	1	
S81916	PGK1	2.0	1	
NM_015393	DKFZP564O0823	2.0	1	
AF257099	PTMA	0.4	1	
NM_002439	MSH3	0.4	1	

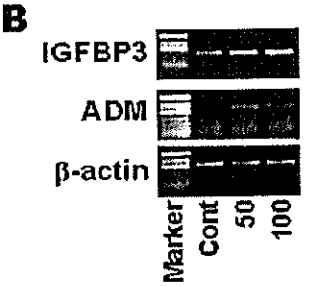

FIGURE 4 - Candidate genes for biomarkers regulated by ZD6474 treatment. Each colored block represents the expression level of a given gene in an individual sample. (*a*) Upregulated genes with a ≥2-fold change or ≤0.5-fold change are shown (mean value in the ZD6474 group/vehicle control group). Cont, vehicle control group, $n = 2$; 50, ZD6474 50 mg/kg/day group, $n = 2$; 100, ZD6474 100 mg/kg/day group, $n = 2$. [1]Number of different probes that passed fold-change criteria above. [2]Reference number for genes whose expression has been reported to be related to hypoxia. [3]Red represents increased expression and blue represents decreased expression relative to the normalized expression of the gene across all samples. (*b*) mRNA expression levels of 2 representative genes, *IGFBP-3* and *ADM*, detected by RT-PCR in tumors treated with ZD6474. *IGFBP-3* and *ADM* mRNA expression was induced in response to ZD6474.

they need by passive diffusion, but angiogenesis is required for the growth of tumors larger than 2 mm.[22] A second possible mechanism is that ZD6474 may inhibit the growth or migration of tumor vascular endothelial cells in "small tumor lesions" by inhibiting VEGFR2-dependent intracellular signaling. This effect would be expected to limit metastatic tumor growth due to lack of oxygen and nutrients, and reduce the dissemination of cancer cells.

To identify putative biomarkers of the pharmacodynamic effects of ZD6474 *in vivo*, we identified 28 candidate genes from implanted 58As1 tumor samples by oligonucleotide microarray analysis (Fig. 4*a*). IGFBP-3 has multiple functions, including in the induction of apoptosis,[23] the inhibition of cancer cell proliferation,[24] and carcinogenesis[25] and IGFBP-3 expression is transcriptionally upregulated under hypoxic conditions.[26] A recent study has also shown that EGFR regulates IGFBP-3 expression and secretion.[27] The inhibitory effect of ZD6474 on EGFR kinase may be associated with the upregulation of IGFBP-3. ADM, which was first identified in a human pheochromocytoma, is known to regulate circulation by acting as a hormone.[28] Adrenomedullin is also induced by hypoxia and may have a role in protecting against hypoxic cellular damage in human retinal pigment epithelial cells.[29] Expressions of nine of the upregulated genes, *IGFBP-3*, *ADM*, *ANGPTL4*, *PLOD2*, *DSIPI*, *NDRG1*, *ENO2*, *HIG2* and *BNIP3L*, has been reported previously to be induced by hypoxia.[26,29–38] We hypothesize that ZD6474 inhibits neovascularization in tumors, thereby limiting the oxygen and nutrient supply and resulting in tumor hypoxia and upregulation of hypoxia-inducible genes. If this hypothesis is correct, hypoxia-regulated genes and gene products might be useful biomarkers for the pharmacodynamic effects of ZD6474 and other anti-angiogenic agents in preclinical and clinical settings. We are now investigating whether these genes and gene products can be used as biomarkers for the efficacy of ZD6474 in a correlative study.

Future directions of our study include: (*i*) to compare the antitumor effect of other "anti-vascular agents" with ZD6474 in this model; (*ii*) to evaluate combination therapy with ZD6474 plus anticancer agents; (*iii*) to evaluate the antitumor effect of ZD6474 against micro-metastasis *in vivo*; and (*iv*) to confirm the usefulness of the 9 candidate genes as biomarkers in clinically.

In conclusion, we demonstrated that ZD6474 inhibited tumor growth, suppressed intraperitoneal dissemination, and prolonged survival in a highly metastatic orthotopic gastric cancer model. We carried out a microarray analysis of tumor samples and we identified 9 hypoxia-inducible genes as candidate biomarkers for monitoring the effects of ZD6474 therapy. These findings provide a strong preclinical rationale for investigating ZD6474 for the treatment of gastric cancer in the clinic.

Acknowledgements

Grants were received from the 3rd-Term Comprehensive 10-Year Strategy for Cancer Control and from a Grant-in-Aid for Scientific Research from the Ministry of Education, Culture, Sports, Science and Technology of Japan (Grant number: 12217165). T.A. is the Recipient of a Research Resident Fellowship from the Foundation of Promotion of Cancer Research in Japan.

References

1. Vanhoefer U, Rougier P, Wilke H, Ducreux MP, Lacave AJ, Van Cutsem E, Planker M, Santos JG, Piedbois P, Paillot B, Bodenstein H, Schmoll HJ, et al. Final results of a randomized phase III trial of sequential high-dose methotrexate, fluorouracil, and doxorubicin versus etoposide, leucovorin, and fluorouracil versus infusional fluorouracil and cisplatin in advanced gastric cancer: A trial of the European Organization for Research and Treatment of Cancer Gastrointestinal Tract Cancer Cooperative Group. J Clin Oncol 2000;18:2648–57.
2. Ohtsu A, Shimada Y, Shirao K, Boku N, Hyodo I, Saito H, Yamamichi N, Miyata Y, Ikeda N, Yamamoto S, Fukuda H, Yoshida S. Randomized phase III trial of fluorouracil alone versus fluorouracil plus cisplatin versus uracil and tegafur plus mitomycin in patients with unresectable, advanced gastric cancer: the Japan Clinical Oncology Group Study (JCOG9205). J Clin Oncol 2003;21:54–9.
3. Moriguchi S, Kamakura T, Odaka T, Nose Y, Maehara Y, Korenaga D, Sugimachi K. Clinical features of the differentiated and undifferentiated types of advanced gastric carcinoma: univariate and multivariate analyses. J Surg Oncol 1991;48:202–6.
4. Ferrara N, Davis-Smyth T. The biology of vascular endothelial growth factor. Endocr Rev 1997;18:4–25.
5. Nicosia RF. What is the role of vascular endothelial growth factor-related molecules in tumor angiogenesis? Am J Pathol 1998;153:11–6.
6. Mustonen T, Alitalo K. Endothelial receptor tyrosine kinases involved in angiogenesis. J Cell Biol 1995;129:895–8.
7. Shibuya M. Vascular endothelial growth factor receptor-2: its unique signaling and specific ligand, VEGF-E. Cancer Sci 2003;94:751–6.
8. Manley PW, Bold G, Bruggen J, Fendrich G, Furet P, Mestan J, Schnell C, Stolz B, Meyer T, Meyhack B, Stark W, Strauss A, et al. Advances in the structural biology, design and clinical development of VEGF-R kinase inhibitors for the treatment of angiogenesis. Biochim Biophys Acta 2004;1697:17–27.
9. Hurwitz H, Fehrenbacher L, Novotny W, Cartwright T, Hainsworth J, Heim W, Berlin J, Baron A, Griffing S, Holmgren E, Ferrara N, Fyfe G, et al. Bevacizumab plus irinotecan, fluorouracil, and leucovorin for metastatic colorectal cancer. N Engl J Med 2004;350:2335–42.
10. Wedge SR, Ogilvie DJ, Dukes M, Kendrew J, Chester R, Jackson JA, Boffey SJ, Valentine PJ, Curwen JO, Musgrove HL, Graham GA, Hughes GD, et al. ZD6474 inhibits vascular endothelial growth factor signaling, angiogenesis, and tumor growth following oral administration. Cancer Res 2002;62:4645–55.
11. Ciardiello F, Caputo R, Damiano V, Troiani T, Vitagliano D, Carlomagno F, Veneziani BM, Fontanini G, Bianco AR, Tortora G. Antitumor effects of ZD6474, a small molecule vascular endothelial growth factor receptor tyrosine kinase inhibitor, with additional activity against epidermal growth factor receptor tyrosine kinase. Clin Cancer Res 2003;9:1546–56.
12. Sandstrom M, Johansson M, Andersson U, Bergh A, Bergenheim AT, Henriksson R. The tyrosine kinase inhibitor ZD6474 inhibits tumour growth in an intracerebral rat glioma model. Br J Cancer 2004;91:1174–80.
13. McCarty MF, Wey J, Stoeltzing O, Liu W, Fan F, Bucana C, Mansfield PF, Ryan AJ, Ellis LM. ZD6474, a vascular endothelial growth factor receptor tyrosine kinase inhibitor with additional activity against epidermal growth factor receptor tyrosine kinase, inhibits orthotopic growth and angiogenesis of gastric cancer. Mol Cancer Ther 2004;3:1041–8.
14. Taguchi F, Koh Y, Koizumi F, Tamura T, Saijo N, Nishio K. Anticancer effects of ZD6474, a VEGF receptor tyrosine kinase inhibitor, in gefitinib (Iressa) sensitive and resistant xenograft models. Cancer Sci 2004;95:984–9.
15. Arao T, Fukumoto F, Takeda M, Tamura T, Saijo N, Nishio K. Small in-frame deletion in the epidermal growth factor receptor as a target for ZD6474. Cancer Res 2004;64:9101–4.
16. Yanagihara K, Tanaka H, Takigahira M, Ino Y, Yamaguchi Y, Toge T, Sugano K, Hirohashi S. Establishment of two cell lines from human gastric scirrhous carcinoma that possess the potential to metastasize spontaneously in nude mice. Cancer Sci 2004;95:575–82.
17. Yanagihara K, Takigahira M, Tanaka H, Komatsu T, Fukumoto H, Koizumi F, Nishio K, Ochiya T, Ino Y, Hirohashi S. Development and biological analysis of peritoneal metastasis mouse models for human scirrhous stomach cancer. Cancer Sci 2005;6:323–32.
18. Lynch TJ, Bell DW, Sordella R, Gurubhagavatula S, Okimoto RA, Brannigan BW, Harris PL, Haserlat SM, Supko JG, Haluska FG, Louis DN, Christiani DC, et al. Activating mutations in the epidermal growth factor receptor underlying responsiveness of non-small-cell lung cancer to gefitinib. N Engl J Med 2004;350:2129–39.
19. Paez JG, Janne PA, Lee JC, Tracy S, Greulich H, Gabriel S, Herman P, Kaye FJ, Lindeman N, Boggon TJ, Naoki K, Sasaki H, et al. EGFR mutations in lung cancer: correlation with clinical response to gefitinib therapy. Science 2004;304:1497–500.
20. Pao W, Miller V, Zakowski M, Doherty J, Politi K, Sarkaria I, Singh B, Heelan R, Rusch V, Fulton L, Mardis E, Kupfer D, et al. EGF receptor gene mutations are common in lung cancers from "never smokers" and are associated with sensitivity of tumors to gefitinib and erlotinib. Proc Natl Acad Sci USA 2004;101:13306–11.
21. Yang SH, Lin JK, Lai CR, Chen CC, Li AF, Liang WY, Jiang JK. Risk factors for peritoneal dissemination of colorectal cancer. J Surg Oncol 2004;87:167–73.
22. Folkman J. What is the evidence that tumors are angiogenesis dependent? J Natl Cancer Inst 1990;82:4–6.
23. Kim HS, Ingermann AR, Tsubaki J, Twigg SM, Walker GE, Oh Y. Insulin-like growth factor binding protein 3 induces caspase-dependent apoptosis through a death receptor-mediated pathway in MCF-7 human breast cancer cells. Cancer Res 2004;64:2229–37.
24. Kirman I, Polyakovskaia N, Sylla P, Whelan RL. Insulin-like growth factor binding protein 3 inhibits growth of experimental colorectal carcinoma. Surgery 2004;136:205–9.

25. Renehan AG, Zwahlen M, Minder C, O'Dwyer ST, Shalet SM, Egger M. Insulin-like growth factor (IGF)-I, IGF binding protein-3, and cancer risk: systematic review and meta-regression analysis. Lancet 2004;363:1346–53.
26. Koong AC, Denko NC, Hudson KM, Schindler C, Swiersz L, Koch C, Evans S, Ibrahim H, Le QT, Terris DJ, Giaccia AJ. Candidate genes for the hypoxic tumor phenotype. Cancer Res 2000;60: 883–7.
27. Takaoka M, Harada H, Andl CD, Oyama K, Naomoto Y, Dempsey KL, Klein-Szanto AJ, El-Deiry WS, Grimberg A, Nakagawa H. Epidermal growth factor receptor regulates aberrant expression of insulin-like growth factor-binding protein 3. Cancer Res 2004;64:7711–23.
28. Hirata Y, Hayakawa H, Suzuki Y, Suzuki E, Ikenouchi H, Kohmoto O, Kimura K, Kitamura K, Eto T, Kangawa K. Mechanisms of adrenomedullin-induced vasodilation in the rat kidney. Hypertension 1995;25:790–5.
29. Udono T, Takahashi K, Nakayama M, Yoshinoya A, Totsune K, Murakami O, Durlu YK, Tamai M, Shibahara S. Induction of adrenomedullin by hypoxia in cultured retinal pigment epithelial cells. Invest Ophthalmol Vis Sci 2001;42:1080–6.
30. Le Jan S, Amy C, Cazes A, Monnot C, Lamande N, Favier J, Philippe J, Sibony M, Gasc JM, Corvol P, Germain S. Angiopoietin-like 4 is a proangiogenic factor produced during ischemia and in conventional renal cell carcinoma. Am J Pathol 2003;162:1521–8.
31. Hofbauer KH, Gess B, Lohaus C, Meyer HE, Katschinski D, Kurtz A. Oxygen tension regulates the expression of a group of procollagen hydroxylases. Eur J Biochem 2003;270:4515–22.
32. Khvatova EM, Samartzev VN, Zagoskin PP, Prudchenko IA, Mikhaleva II. Delta sleep inducing peptide (DSIP): effect on respiration activity in rat brain mitochondria and stress protective potency under experimental hypoxia. Peptides 2003;24:307–11.
33. Cangul H. Hypoxia upregulates the expression of the NDRG1 gene leading to its overexpression in various human cancers. BMC Genet 2004;5:27.
34. Szturmowicz M, Burakowski J, Tomkowski W, Sakowicz A, Filipecki S. Neuron-specific enolase in non-neoplastic lung diseases, a marker of hypoxemia? Int J Biol Markers 1998;13:150–3.
35. Denko N, Schindler C, Koong A, Laderoute K, Green C, Giaccia A. Epigenetic regulation of gene expression in cervical cancer cells by the tumor microenvironment. Clin Cancer Res 2000;6:480–7.
36. Kenny PA, Enver T, Ashworth A. Receptor and secreted targets of Wnt-1/beta-catenin signalling in mouse mammary epithelial cells. BMC Cancer 2005;5:3.
37. Fei P, Wang W, Kim SH, Wang S, Burns TF, Sax JK, Buzzai M, Dicker DT, McKenna WG, Bernhard EJ, El-Deiry WS. Bnip3L is induced by p53 under hypoxia, and its knockdown promotes tumor growth. Cancer Cell 2004;6:597–609.
38. Sowter HM, Ratcliffe PJ, Watson P, Greenberg AH, Harris AL. HIF-1-dependent regulation of hypoxic induction of the cell death factors BNIP3 and NIX in human tumors. Cancer Res 2001;61: 6669–73.

Acta Med Kinki Univ Vol. 31, No. 2, 57-62, 2006

Progress in the field of molecular biology and application of biotechnology to medical oncology

Kazuto Nishio and Tokuzo Arao

Department of Genome Biology, Kinki University School of Medicine, Osakasayama, Osaka 589-8511, Japan

Abstract

Recent progress in the field of molecular biology has been expected to contribute to progress in the field of clinical medicine. Personalized medicine could be achieved by pharmacogenomics. Prospective clinical studies using biomarkers are considered to be important. Investigators should plan the study design and carefully perform such studies.

Key words: Pharmacogenomics, DNA chip, biomarker, prediction

Introduction

Remarkable progress has been made in the field of molecular biology in the 20th century (Table 1). The entire human genome has been sequenced by the Human Genome Project. The 21st century is, therefore, called the "Post Genome" era and further advances in the clinical application of biotechnology are expected. Applied biotechnology is also useful for both diagnostic and therapeutic oncology. Here, we shall discuss the application of biotechnology to the field of medical oncology.

Table 1 Progress in the field of molecular biology during the 20th century

year	event
1890	Mendelism
1926	Genes on chromosome (Mogan)
1944	DNA as gene component (Fibree)
1953	Double helix of DNA (Watson & Crick)
1956	Replication enzyme of DNA (Komburg)
1973	Recombination technology (Cohen)
1985	PCR (Mullis)
1990	Start the Human Genome Project
1998	Deciphering the human genome proceed to multicellular organism
2001	Decoding of the human genome by Celera Genomics Co.

Tissue Banking

Genome biology is expected to be applied to drug development. Drug development, such as that of cytotoxic anticancer drugs and molecular target drugs in the field of oncology, is one of the most upcoming fields. The first and most important step of drug screening is target identification and the search for seeds. The next step is screening of the compounds, followed by preclinical and clinical studies. It is considered that genomic information effectively contributes to the target identification and its validation. To obtain data about the human genome, analysis of human materials is essential. This approach is called the "Reverse Translational Research". In the clinical setting, it is also called "Molecular Correlative Study". These approaches are adopted by government-supported projects both in Japan and abroad. Pharmaceutical companies also aggressively conduct a search for seeds. Mega-pharmas, in particular, have already established the banking system for human materials. Japan has also started a banking system, but it seems to be still immature and Japan still falls behind other countries. The process of collecting clinical samples is called "Tissue Banking" or simply "Banking".

Pharmacogenomics

The approach mentioned above is also applied in the clinical setting. One of the well-recognized approaches is "Personalized Medicine,"

that allows therapy to be customized to individuals by analyzing the individual's genome. Analysis of the genome is called "pharmacogenomics" when it is related to treatment with drugs "Pharmacogenomics" is a word combining "genomics" and "pharmacology" Broadly, pharamcogenomics includes the analysis of gene products, such as RNA and proteins The pharmacogenomic approach is considered to contribute to health and welfare. The US and other governments are encouraging this strategy. For example, the US government provides guidance to the industry on the process of Investigational New Drug (IND), New Drug Application (NDA), and Biologic Licence Application (BLA). In our country, the Ministry of Health, Welfare, and Labour has requested for genomic information obtained by the genomic testing in clinical studies for pharmaceutical companies.

Application of pharamcogenomics is expected in three major stages : discovery, preclinical, and clinical stages (Table 2). Three examples are provided as follows ; i) research on gene-related diseases ; ii) relationship between gene polymorphism and response to drug treatment ; iii) genomic tests for the prediction of drug responses. Examples 2 and 3 are considered to be closely associated with cancer treatment and will directly contribute to the exclusion of patients with severe toxicities or to the selection of responders and non-responders to a particular treatment. The markers obtained by pharmacogenomics are called as "biomarkers".

Biomarkers for molecule-targeting drugs

We would like to consider biomarkers for target-based drugs. 1) Overexpression of the target molecule ; this is often detected by immunohitochemical analysis. Amplification of target molecules is detected by FISH, CISH or PCR Somatic mutations in tumor tissues are detected by direct sequencing or other PCR-based assays. For the purification of tumor tissues, the microdissection technique is useful There are biomarkers for conventional cytotoxic drugs ERCC1 is an enzyme involved in DNA repair and its transcript levels have been reported to be related to the responses to platinum-containing regimens (e.g., cisplatin plus gemicitabine) in non-small cell lung cancer patients.[1] Thus, biomarkers could be determinants for predicting the sensitivity and responses of tumors to cytotoxic drugs.

As mentioned above, the EGFR somatic mutation in lung cancer is a hot topic. Strong correlation has been observed between EGFR somatic mutations and clinical responses to an EGFR-specific tyrosine kinase inhibitor, gefitinib. Thus, the EGFR mutation is a definite biomarker, and other somatic mutations of oncogenes in tumors have been also reported. These mutations could be used as new biomarkers to clarify subpopulations of patients that would respond to molecule-targeting drugs. Currently, trials for new molecule-targeting therapeutics are now underway for solid tumors. Treatment with angiogenesis inhibitors and antibodies are expected to improve the outcome of patients. New biomarkers need to be continually sought for this type of therapeutics.

Now, these molecular correlative studies are called as "Critical Path Research" in the field of drug development (Fig. 1).

Considering the background of aggressiveness of biomarker research, the average response to drugs is much lower than that of other diseases (Fig. 2)

The average response rate to anticancer drugs is 20-30%, which is inadequate. In order to improve the response rate to anticancer drugs, selection of subpopulations of patients that

Table 2 Three broad applications of pharmacogenomics

Discovery
Target identification
Mechanisms of Action
Target differentiation
Biomarker identification
Preclinical Toxicology
Toxicogenomics
In vivo mechanism of action
Biomarker identification
Clinical
In vivo mechanism of action
Biomarker development and validation

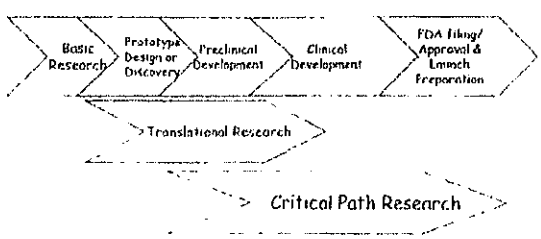

Fig. 1 Critical path Significant benefit of bringing innovative products faster to the public

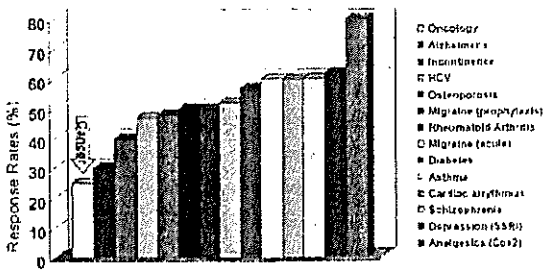

Fig. 2 The need for better predictive markers (Paul Warning, Genentech, modified)

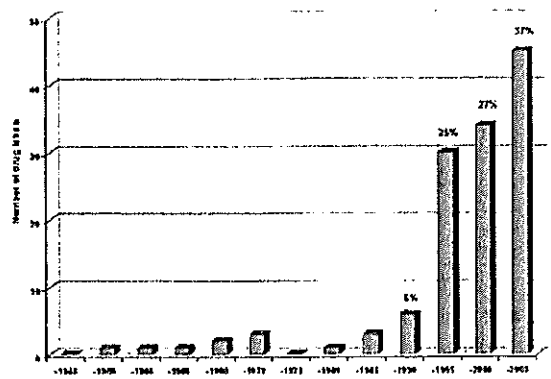

Fig. 3 Labels of approved drugs with pharmacogenomic information (Frueh FW, CDER/FDA, modified)

would potentially show response is one strategy. At the same time, the labeling of drugs with pharmacogenomic data has been increasing recently (Fig. 3)

Government-related regulatory institutions in the US (Department of Health and Human Services, Food and Drug Administration, Center for Drug Evaluation and Research (CDER), Center for Biologic Evaluation and Research (CBER), Center for Devices and Radiological Health (CDRH)) developed a "Guideline for Industry," by which pharmaceutical companies are required to submit pharmacogenomic data. How should investigators assess/evaluate the data? Essentially, we should recognize three categories of pharmacogenomic information while selecting the treatment strategy: 1) test required, 2) test recommended, 3) information only.

Trastuzumab (Herceptin®) for breast cancer is a good example of the first; testing for anti-Her2 by FISH analysis (Hereceptest®) is required for the administration of Trastuzumab. Although EGFR somatic mutation, EGFR immunohistochemistry, and FISH for EGFR are considered to be good biomarkers for predicting the response to EGFR-targeting drugs, they belong to the "Test only" category. It is not within the scope of this review to discuss why these differences exist. Anyway, applied pharmacogenomics is very important in the selection of appropriate subpopulations, and an increase in the number of "Test required" biomarkers is warranted.

Another point for discussion is that the pharmacogenomic approach has so far focused on the prediction or evaluation of adverse events. Single- nucleotide polymorphisms of metabolizing enzymes, such as p450 or UDP-glucuronoyltransferases (UGT)[2] are closely related to the toxicity profile of drugs. Therefore, tests for these genes are also included in the label of the drugs. The available evidence actually contributes to identify subpopulations of patients likely to show severe side effects. On the other hand, there is not much evidence, in terms of biomarkers, to distinguish accurately between responders and non-responders. It is important to consider the latter approach when considering personalized medicine.

Drug-diagnostic co-development

As mentioned before, the importance of pharmacogenomics has been discussed worldwide. Last year, the FDA proposed the new concept "drug-diagnostic co-development", although it is still in the draft stage and needs open discussion. What is the "co-development"? "Co-development" means: 1) Critical Path Research for biomarkers that would distinguish responders from non-responders in clinical studies; 2) research for avoiding severe toxicities; 3) clinical studies for POC (proof of concept) by monitoring pharmacodynamic markers. The endpoints of these approaches are to set the appropriate doses for each subpopulation or responders. Investigators should consider the study designs flexibly in these approaches. For example, randomized phase II studies and randomized discontinuation studies may be given more consideration. In addition, for the selection of biomarkers in Critical Path Research, more strict validation will be necessary, because the tests using the biomarkers will directly affect the treatment of each patient.

Problems in pharamcogenomics and future perspectives

Biomarker researches can be divided into two categories, "hypothesis-driven" and "hypothesis-free"; the former is to prove the power of preex-

isting biomarkers (predictability, reliability, specificity e.g.), whereas the latter is to select biomarkers without any hypothesis, by DNA microarray or proteomics. At the same time, validation of the selected biomarkers is necessary. Currently, the hypothesis-free approach seems to be the trend.

In general, biomarkers in the hypothesis-driven approach are relatively easy to understand, and are based on biological evidence. They can be expected to be more easily applied clinically. However, there is a limitation: only pre-existing biomarkers can be used. On the other hand, in the case of biomarkers in the hypothesis-free approach, it is difficult to understand underlying biological mechanisms and it is difficult to directly apply these markers clinically. However, novel biomarkers can be discovered by this approach.

When considering a new prospective study using microarray gene expression profiling, it is of importance to pay attention to some points, as follows. The investigators should recognize the role of quality assurance and perform the study accordingly. Regarding the data of DNA expression for Cancer Diagnostics, the guidelines proposed by the NCI-EORTC Working Group are helpful.[3] For the development of classifications based on the gene expression profile, the following points must be taken into consideration. 1) A common therapy is essential for identical populations. Are the results reasonable enough to establish a therapeutic policy? Will the new classification be generally used based on the cost-benefit balance, by comparing the selection of the therapies and the cost for mis-classified? These points should be discussed preliminarily during the process of designing of the study. For further evaluation, internal validation is necessary to prove the accuracy of the new classification in comparison with the pre-existing prognostic factors. The validation process includes 1) transfer to other platforms that are commonly used in clinical situations. (For example, will the classification identified by DNA chip analysis be valid for transfer to that by RT-PCR or immunohistochemical (ICH) examination), 2) confirmation of the reproducibility of the classification by the new platform (RT-PCR or ICH), and 3) independent validation in a prospective study. In addition, the investigators should recognize "multiplicity" of the comprehensive data sets, such as those of gene expression. Many researchers have reported classifiers to predict the prognosis of patients with cancers. For example, a 17- gene signature associated with metastasis was identified by a DNA chip analysis by Ramaswamy et al.,[4] (Fig. 4)

Several researchers have attempted the same

Table 3 The 17 gene signature associated with metastasis

Gene	Gene name	GenBank ID
Upregulated in metastases		
SNRPF	Small nuclear ribonucleoprotein F	A1032612
EIF4EL3	Elongation initiation factor 4E-like 3	AF038957
HNRPAB	Heterogeneous nuclear ribonucleoprotein A/B	M65028
DHPS	Deoxyhypusine synthase	U79262
PTTG1	Securin	AA203476
COL1A1	Type I collagen, α1	Y15915
COL1A2	Type I collagen, α2	J03464
LMNB1	Lamin B1	L37747
Downregulated in metastases		
ACTG2	Actin, γ2	D00654
MYLK	Myosin light chain kinase	U48959
MYH11	Myosin, heavy chain 11	AF001548
CNN1	Calponin 1	D17408
HLA-DPB1	MHC Class II, DPβ1	M83664
RUNX1	Runt-related transcription factor 1	D43969
MT3	Metallothioncin 3	S72043
NR4A1	Nuclear hormone receptor 1R3	L13740
RBM5	RNA binding motif 5	AF091263

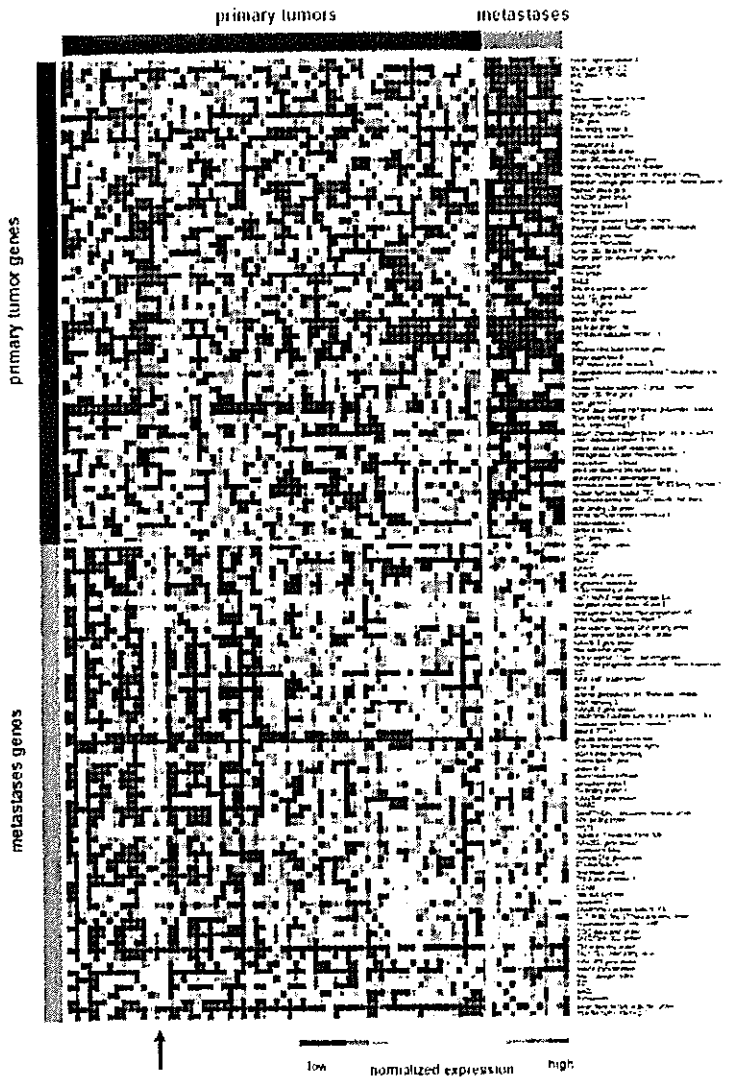

Fig. 4 Genes associated with metastases.
Columns represent human tumor samples (64 primary and 12 metastatic adenocarcinomas), rows represent the 128 genes (64 overexpressed and 64 underexpressed in metastases) that best distinguished the primary from the metastatic tumors using a weighted voting algorithm in leave-one-out cross-validation (cross-validation accuracy = 80%, $P = 0.012$ by permutation testing; Colorgram depicts high (red) and low (blue) relative levels of gene expression. A 'striped' pattern was observed in some primary tumors (arrow), indicating the presence of a gene-expression program associated with metastases. *(Ramaswamy et al., Nature Genetics 2002)*

approach and obtained gene sets that predict prognosis of patients with breast cancer. Sorlie selected a set of 456 genes[5] (PNAS 2001). Van't Veer selected a set of 231 genes determining the prognosis and validated it using the independent data of 295 patients.[6] However, in relation to their selected genes, a few genes were overlapped. This discrepancy might be due to the following reasons: 1) validation in different clinical backgrounds, such as disease, histology, response criteria, and treatment, 2) difference in the assay methods used for RNA purification and in the methods used for gene amplification, and/or 3) difference in the analytical process used, such as standardizations and algorithms. How should future biomarker studies be considered? Future biomarker studies should include: 1) a prospective correlative study between markers and clinical features (survival and response e.g.), 2) barebones sample size, and 3) validation on another platform.[7]

Another problem is that the selected markers

usually contain many functionally unknown markers. Therefore, it is difficult to discuss the implications of biomarkers without the availability of biological information. At the same time, it is necessary to analyze the functions of each biomarker, which requires much effort. Therefore, investigators should start biomarker (pharmacogenomic) studies in the early phase. Statistically, algorithms and data sets containing the biological information should be constructed. In addition, standardization of these analytical methods is essential. For clinical side application ?, adequate prospective clinical studies are required. It is thus of utmost importance to establish better communication between clinical researchers, basic researchers and bio-statisticians from the planning stage.

References

1. Olaussen KA, Dunant A, Fouret P, Brambilla E, Andre F, Haddad V, Taranchon E, Filipits M, Pirker R, Popper HH, Stahel R, Sabatier L, Pignon JP, Tursz T, Le Chevalier T, Soria JC ; IALT Bio Investigators (2006) DNA repair by ERCC1 in non-small-cell lung cancer and cisplatin-based adjuvant chemotherapy. N Engl J Med 355 : 983 991
2. Innocenti F, Undevia SD, Iyer L, Chen PX, Das S, Kocherginsky M, Karrison T, Janisch L, Ramirez J, Rudin CM, Vokes EE, Ratain MJ (2004) Genetic variants in the UDP-glucuronosyltransferase 1A1 gene predict the risk of severe neutropenia of irinotecan. J Clin Oncol 22 : 1382 1388
3. McShane LM, Altman DG, Sauerbrei W, Taube SE, Gion M, Clark GM (2005) Statistics Subcommittee of the NCI-EORTC Working Group on Cancer Diagnostics. J Clin Oncol 23 : 9067-9072
4. Ramaswamy S, Ross KN, Lander ES, Golub TR (2003) A molecular signature of metastasis in primary solid tumors. Nat Genet 33 : 49 54
5. Sorlie T, Tibshirani R, Parker J, Hastie T, Marron JS, Nobel A, Deng S, Johnsen H, Pesich R, Geisler S, Demeter J, Perou CM, Lonning PE, Brown PO, Borresen-Dale AL, Botstein D (2003) Repeated observation of breast tumor subtypes in independent gene expression data sets. Proc Natl Acad Sci U S A. 100 : 8418 8423
6. van de Vijver MJ, He YD, van't Veer LJ, Dai H, Hart AA, Voskuil DW, Schreiber GJ, Peterse JL, Roberts C, Marton MJ, Parrish M, Atsma D, Witteveen A, Glas A, Delahaye L, van der Velde T, Bartelink H, Rodenhuis S, Rutgers ET, Friend SH, Bernards R (2002) A gene-expression signature as a predictor of survival in breast cancer. N Engl J Med. 347 : 1999-2009
7. Simon R (2005) Roadmap for developing and validating therapeutically relevant genomic classifiers. J Clin Oncol 23 : 7332 7341

Acta Med Kinki Univ Vol. 31, No. 2, 67 74, 2006

Development and characterization of an antibody specifically recognizing a mutant EGFR (L858R) protein expressed frequently in non-small cell lung cancer

Makoto Kawaishi*, Hideyuki Yokote**, Hideharu Kimura***, Kazuo Kasahara*** and Kazuto Nishio*,**

*Shien-Lab, National Cancer Center Hospital, National Cancer Center Research Institute, 5-1-1 Tsukiji, Chuo-ku, Tokyo, Japan
**Department of Genome Biology, Kinki University School of Medicine, Osakasayama, Osaka, 589-8511, Japan
***Respiratory Medicine, Kanazawa University Hospital, 13-1 Takara-machi, Kanazawa, Ishikawa, Japan

Abstract

L858R point mutation in exon 21 of the EGFR gene, accounting for approximately 40% of non-small cell lung cancer (NSCLC)-associated EGFR mutations, has been known to hyper-respond to gefitinib, a selective EGFR tyrosine kinase inhibitor. From this view point, it is important to detect EGFR mutations. Immunohistochemistry (IHC) is commonly used to analyze the molecular status of several clinical specimens. We have developed specific antibodies recognizing the mutant EGFR (L858R) protein and characterized the antibodies by ELISA, Western blot, immunocytochemistry, and immunohistochemistry. Using any of these evaluation methods, we found an antibody, AbyD02889, which could detect the EGFR (L858R) protein with specificity. AbyD02889 may be a useful tool to detect the EGFR (L858R) mutation of NSCLC in the clinical situation. IHC using the mutant-specific anti-EGFR antibody will be a powerful assay to predict or select subpopulation sensitive to EGFR-TKI.

Key words: NSCLC, mutant EGFR, HuCAL antibody

Introduction

Lung cancer is a major cause of cancer-related mortality worldwide and is expected to remain a major health problem for the foreseeable future.[1] Targeting the epidermal growth factor receptor (EGFR) is one appealing therapeutic strategy for non-small cell lung cancer (NSCLC) because constitutively-active types of EGFR mutations, sometimes together with their strong expression, have been believed to contribute to the pathological features of NSCLC such as disease progression, or unregulated cell growth.[2] In the clinical situation, NSCLC tumors with such mutations have been reported to hyper-respond significantly to gefitinib, a selective EGFR tyrosine kinase inhibitor.[3,4] Such EGFR mutations consisted of small in-frame deletions or substitutions clustered around the ATP-binding site in exons 18, 19, and 21 of the EGFR, and the mutations increased the affinity of the enzyme for ATP and gefitinib. Some investigators subsequently found that these EGFR mutations were strong determinants of the tumor response to an EGFR tyrosine kinase inhibitor.[5-7] The two studies demonstrated two major EGFR mutations (E746 A750del in exon 19 and L858R in exon 21) occupying approximately 90% of the NSCLC-

Received October 23, 2006, Accepted November 10, 2006

associated EGFR mutations, in both trials using surgical tissue to detect the EGFR mutations.[8,6]

Our laboratory has also been interested in the clinical relationship between the somatic EGFR mutations and responsiveness of NSCLC-tumors to EGFR tyrosine kinase inhibitors. Kilmura reported that the Scorpion ARMS method could detect the EGFR mutations using serum or pleural effusion from NSCLC patients with a high sensitivity, reliability, and less invasiveness even though only a small amount of genomic DNA was contained in the serum or pleural effusion sample.[9,10] In addition to these approaches to detect EGFR mutations using genomic DNA, it is considered important and useful to specifically detect the mutant EGFR proteins which are final products by the somatic mutations in cancer cells. From this view point, development of a specific antibody recognizing a mutant EGFR protein becomes a useful alternative method of detection to PCR-based genomic diagnosis, which will provide us with even more information about the mutation. For example, using the mutant-specific antibody and immunocytochemical technique, we will be able to conveniently detect EGFR mutations in only one cancer cell.

MorphoSys (Munich, Germany) provides an uniquely powerful technology of antibody generation. In the HuCAL® libraries, the structural diversity of the human antibody repertoire is represented by seven heavy chain and seven light chain variable region genes, giving rise to 49 frameworks in the master library. Highly variable genetic cassettes (CDRs, complementarity determining regions) are then superimposed on these frameworks to mimic the entire human antibody repertoire (Figure 1A). More than 10 billion functional human antibody specificities in Fab format have already been prefabricated and are available in phage libraries.[11-13]

Using this technology, we developed a specific antibody for the mutant EGFR (L858R). Herein we report the characterization of the antibody and discuss the feasibility of using the antibody for NSCLC.

Materials and Methods

Expression constructs

A eukaryotic expression vector, pcDNA3.1 (+) (Invitrogen, Carlsbad, CA), was used as a backbone vector to produce pcDNA-IG, which was constructed by insertion of an IRES-EGFP (enhanced green fluorescence protein following internal ribosome entry sequence) fragment at the NotI-XhoI sites of pcDNA3.1 (+). pcDNA-IG expressed the gene of interest together with EGFP and allowed us to ascertain the protein expression indirectly by monitoring the EGFP expression. Full length cDNA of wild-type EGFR and its mutant EGFR (L858R) were amplified by RT-PCR from a human embryonal kidney cell line (HEK293) and a non-small cell lung cancer cell line,[14-16] respectively. A High Fidelity RNA PCR Kit (TaKaRa, Shiga, Japan) was used for the RT-PCR and the following primer sets were synthesized (forward, CGCTAGCCCCCTGACTCCGTCCAGTATTGA; reverse, CCCCTGACTCCGTCCAGTATTGA). The PCR products were amplified again using PyrobestTM DNA polymerase (TaKaRa) with the primer sets (forward, CGCTAGCCCCCTGACTCCGTCCAGTATTGA; reverse, CGAAGCTTTGCTCCAATAAATTCACTGC). This amplified DNA encoding wild-type and mutant EGFR included NheI and HindIII at the 5'- and 3'-ends, respectively. These two PCR products were subcloned into a pCR BluntII-TOPO vector (Invitrogen) and their sequences were confirmed with an ABI 310 capillary sequencer (Applied Biosystem).

Reverse and forward oligonucleotides encoding the myc-tag sequence (EQKLISEEDLN) were designed and synthesized as follows: forward, AGCTTGAACAGAAGCTGATCTCAGAGGAGGACCTGAATTGAC; reverse, TCGAGTCAATTCAGGTCCTCCTCTGAGATCAGCTTCTGTTCA. Two oligos were annealed under at the following conditions: 95°C for 2 min, 80°C for 2 min, 55°C and 37°C for 2 min. This annealing procedure generated the ds-oligos including HindIII- and NotI-cut cohesive ends, at the 5'- and 3'-ends, respectively. These ds-oligos were inserted in the HindIII-NotI sites of pcDNA-IG. Subsequently, each cDNA of wild-type or mutant EGFR, that was cut out from the pCR BluntII-TOPO vector with NheI and HindIII, was transferred to the NheI-HindIII sites of pcDNA-IG. Finally, two vectors expressing myc-tagged wild-type or mutant EGFR proteins with EGFP were constructed and designated as pcDNA-EGFR (WT)-myc-IG and pcDNA-EGFR (L858R)-myc-IG, respectively.

Cell culture and transfection

HEK293 (a human embryonal kidney cell line) and H1-18 (a non-small cell lung cancer cell line) cells were maintained in RPMI-1640 medium supplemented with 10 % fetal bovine serum (FBS). pcDNA-EGFR (WT)-myc-IG or pcDNA-EGFR (L858R)-myc-IG was transfected into the HEK293 cells using the FuGene6 transfection reagent (Roche Diagnostics, Basel, Switzerland). Briefly, 80% confluent cells cultured on a 10 cm dish were transiently transfected with 6 μg of vector. Forty-eight hours after transfection, the cells were washed with phosphate buffered saline (PBS) and the cell lysates were prepared for immunoblotting analysis. For immunostaining, the transfected cells were trypsinized once, replated on a poly-L-lysine (PLL) (SIGMA-ALDRICH, St. Louis, MO)-coated 24 well plate, and then used for the examination

ELISA

The specificity of each HuCAL antibody (AbyD02889, AbyD02890, AbyD02991) was checked by ELISA. Briefly, a 96-well microtiter plate was coated with 20 μg/ml of EGFR (WT), EGFR (L858R), CD33-6xHis, Ubiquitin, Stat, and FITC proteins which were diluted in PBS with or without either transferring (Trf) or bovine serum albumin (BSA). After incubation at 37°C for 1 h, the plate was washed three times with PBS. Then, the proteins were proved with each HuCAL antibody at 1 ug/ml followed by incubation with horseradish peroxidase (HRP)-conjugated anti-His antibody (Santa Cruz Biotechnologies). One hundred μl of the substrate solution were added per well. After sufficient color development, 100 μl of stop solution to the wells. The absorbance of each well was read at 450 nm with a plate reader.

Immunoprecipitation and Immunoblotting

The two GST-fused recombinant proteins with cytoplasmic wild-type EGFR and its L858R mutant were purchased from Upstate Biotech (Lake Placid, NY). The transiently transfected HEK293 cells with either pcDNA-EGFR (WT)-myc-IG or pcDNA-EGFR (L858R)-myc-IG were lysed 48 h later with a lysis buffer containing 1% triton X, 50 mM HEPES (pH 7.4), 5 mM EDTA, 50 mM NaCl, 10 mM Na pyrophosphate, 50 mM NaF, 1 mM Na orthovanadate, and protease inhibitor mix, complete™ (Roche). Five hundred micrograms of cell lysate were immunoprecipitated by incubation with 2 μg of anti-myc antibody (Roche) for 3 h followed by further incubation with protein-G agarose (Santa Cruz Biotechnologies) for 1 h. The recombinant proteins and immunoprecipitated samples were separated with SDS-PAGE and blotted on a PVDF membrane. The membrane was probed with HuCAL antibodies, monoclonal anti-EGFR antibody (Cell Signaling, Beverly, MA), or monoclonal anti-pY20 antibody (Cell Signaling) followed by incubation with a monoclonal or polyclonal HRP-conjugated second antibody (Cell Signaling, Beverly, MA). An ECL detection system was then used for visualization. GST-tagged cytoplasmic wild-type and mutant EGFR (L858R) proteins were purchased from Upstate Biotech. For probing with His-tagged anti-EGFR (L858R) HuCAL antibodies, a monoclonal HRP-conjugated anti-His antibody (Santa Cruz Biotechnologies) was used as the second antibody.

Immunocytochemistry and Immunohistochemistry

The H1-18 and HEK293 cells were plated on a PLL-coated 24-well plate at 5,000 cells/well. For assay of the transfected cells, the 48 h-incubated cells after transfection were trypsinized and replated. The cells were fixed with 4% paraformaldehyde for 30 min. The cells were then permeabilized and blocked with a PBS buffer containing 0.3% Triton X and 10% normal goat serum for 1 h and probed with the HuCAL antibodies at 20 μg/ml followed by visualization using an FITC- or rhodamine-conjugated anti-His antibody (Santa Cruz Biotechnologies) as the second antibody. Fluorescence microscopic examination was carried out using a KEYENCE microscopic system (Woodcliff Lake, NJ). For immunohistochemistry, an HRP-conjugated anti-His antibody was used as the second antibody followed by DAB staining.

Results

Generation of monoclonal antibodies against mutant EGFR (L858R)

We used the recombinant antibodies technology provided by MorphoSys (MorphoSys). An antigen (the peptide of mutant EGFR (L858R)) was designed and synthesized. The antigen was screened against the HuCAL GOLD® library (MorphoSys) with its more than 15 billion antibody specificities, which enabled us to develop monoclonal antibodies rapidly. The antigen enters the automated panning process

(AutoPan®, provided by MorphoSys), where it is immobilized for screening against an antibody-displaying phage. Three candidates (AbyD02889, AbyD02890, and AbyD02891) from the screening process were obtained and affinity-purified. We used the monovalent format of the Fab fragment tagged with Myc-His at the C-terminus (Figure 1A) and checked the specificity of these three antibodies with an ELISA for EGFR (WT), EGFR (L858R)-BSA, and EGFR (L858R)-Trf (Figure 1B). Two antibodies, AbyD02889 and AbyD02890, recognized EGFR (L858R) specifically, whereas AbyD02891 bound to both the wild-type and mutant EGFR.

Specificity of HuCAL antibodies against recombinant GST-fused wild type and mutant EGFR proteins

Figure 2A shows a schematic representation of the cytoplasmic domains of wild-type and L858R-mutant EGFR fused with glutathione S-transferase (GST). Using these two antigens, we tested the specificity of the HuCAL antibodies. Both AbyD02889 and AbyD02890 antibodies

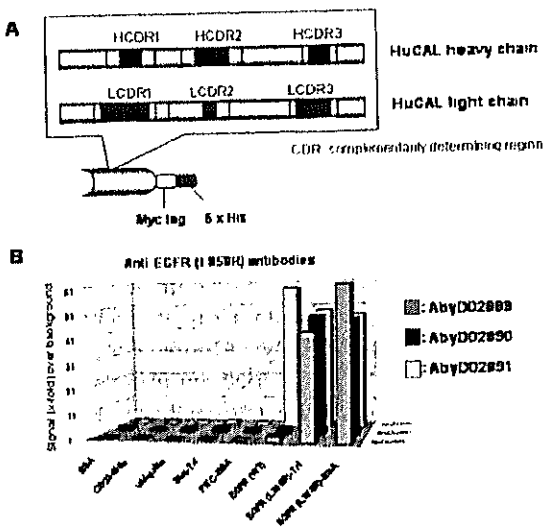

Fig. 1 Generation of monoclonal antibodies against a mutant EGFR (L858R)
(A) A representation of the structure of anti EGFR (L858R) antibodies. The structural diversity of the human antibody repertoire is represented by heavy and light chain variable region genes. Highly variable genetic cassettes (CDRs: complementarity determining regions) are then superimposed on these frameworks to mimic the entire human antibody repertoire. The monovalent format of the Fab fragment we used is tagged with Myc-His at the C-terminus. (B) Characterization of three candidates (AbyD02889, AbyD02890, and AbyD02891) by ELISA. The specificity of the three was checked by an ELISA for EGFR (WT), EGFR (L858R)-BSA, and EGFR (L858R)-Trf.

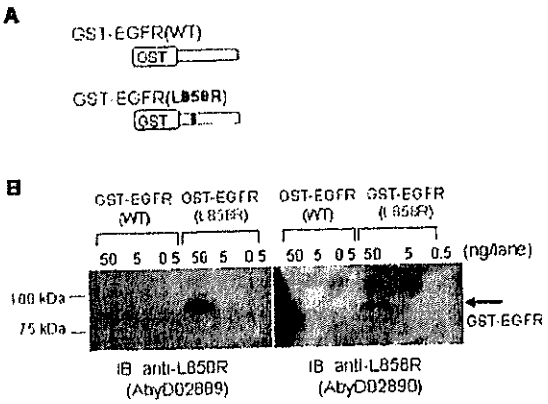

Fig. 2 Immunoblot analysis of two recombinant GST-fused EGFR proteins, GST-EGFR(WT) and GST-EGFR(L858R), using AbyD02889 and AbyD02890.
(A) Cytoplasmic domains of wild-type and L858R-mutant EGFR were fused with glutathione S-transferase (GST) and used for immunoblot analysis as the antigens against AbyD02889 and AbyD02890.
(B) Checking the specificity and affinity of AbyD02889 and AbyD0289050 against two GST-fused EGFR proteins. Fifty, 5, and 0.5 ng of each protein were separated by SDS-PAGE and blotted on a PVDF membrane followed by probing using AbyD02889 or AbyD02890 antibody at 5 μg/ml

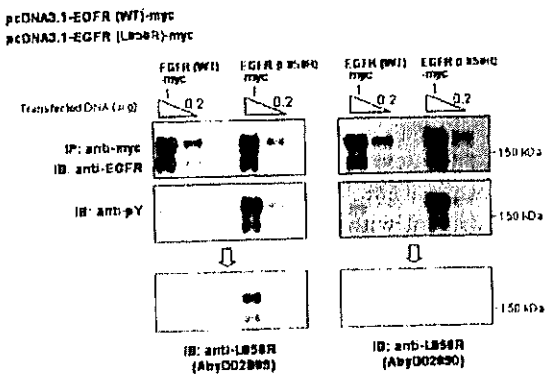

Fig. 3 Checking the specificity and affinity of AbyD02889 and AbyD02890 against the full length wild-type or L858R mutant EGFR protein expressed in the HEK293 cells. One or 0.2 μg of either pcDNA3.1-EGFR (WT)-myc or pcDNA3.1-EGFR (L858R)-myc were transiently transfected into the HEK293 cells (2×10^6 cells/6 cm well). Five hundred μg of cell lysate were immunoprecipitated with anti-myc followed by immunoblotting. The membrane was probed with a commercially available anti-EGFR antibody, anti-pY antibody, AbyD02889 or AbyD02890.

recognized 50 ng mutant EGFR protein specifically, while they were not able to bind to wild-type EGFR protein at all (Figure 2B). In addition, the affinity of AbyD02889 for the mutant protein was clearly demonstrated to be higher than that of AbyD02890.

Specific recognition of AbyD02889 against the full length mutant EGFR (L858R) protein expressed in HEK293 cells

One or 0.2 μg of either pcDNA3.1-EGFR (WT)-myc or pcDNA3.1-EGFR (L858R)-myc was transiently transfected into the 2×10^6 HEK293 cells/6 cm well. Immunoprecipitated EGFR (L858R) protein with anti-myc antibody (in the upper panels of Figure 3) was phosphorylated at a much higher rate than wild-type EGFR protein (in the middle panels). After denuding the anti-pY antibody, the membrane was reproved with AbyD02889 and AbyD02890. AbyD02889 specifically recognized the EGFR (L858R) protein but AbyD02890 did not (in the lower panels). These findings together with the results in Figure 2 suggested that AbyD02889 specifically recognized the EGFR (L858R) protein either produced in bacteria or expressed in human cells.

Immunocytochemical evaluation of the specificity of AbyD02889 and AbyD02890

Next, we checked the feasibility of the use of HuCAL antibodies for immunocytochemistry. The HEK293 cells were transfected with pcDNA3.1 (Figure 4, panels a, d, g, and j), pcDNA3.1-EGFR (WT)-myc (Figure 4, panels b, e, h, and k), or pcDNA3.1-EGFR (L858R)-myc (Figure 4, panels c, f, I, and l). EGFR (L858R)-transfected HEK293 cells (293-L858R) were positive for AbyD02889 (Figure 4, panel c) but negative for AbyD0890 (Figure 4, panel i), and EGFR (WT)-transfected cells were negative for both antibodies (Figure 4, panels b and h). Then, we analyzed H-18 cells harboring an intrinsic EGFR (L858R) mutation using AbyD02889. The H-18 cells were positive for AbyD02889 (Figure 5, panel b) but the HEK293

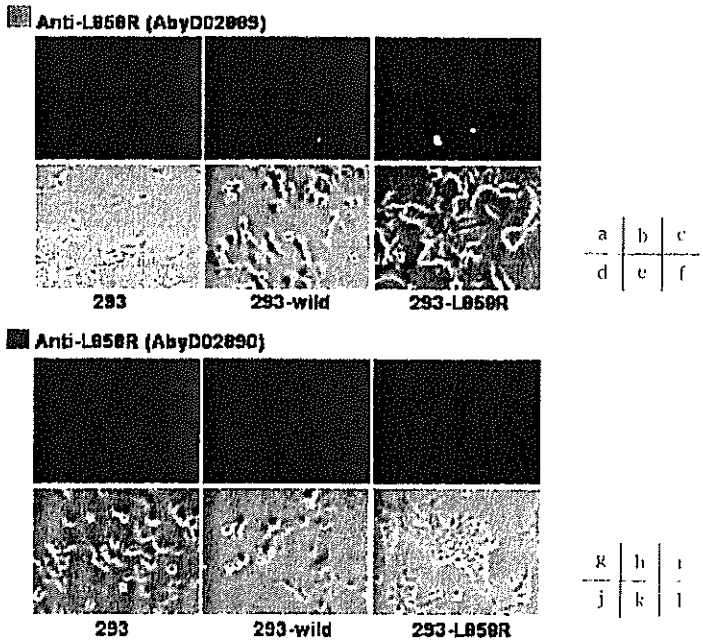

Fig. 4 Evaluation of the specificity of AbyD02889 and AbyD02890 by immunocytochemical analysis. The HEK293 cells transfected with pcDNA3.1 (a, d, g, and j), pcDNA3.1-EGFR (WT)-myc (b, e, h, and k), or pcDNA3.1-EGFR (L858R)-myc (c, f, I, and l) were examined immunocytochemically using the HuCAL antibodies. Forty eight h after transfection, the cells were replated on a PLL-coated 24-well plate at 5,000 cells/well and further incubated for 24 h. After fixation, permialization, and blocking, the cells were probed with the HuCAL antibodies followed by visualization using a rhodamine-conjugated anti His antibody as the second antibody. A fluorescence microscopic examination was carried out. The fluorescence microscopic views of the cells probed with AbyD02889 and AbyD02890 are shown in the upper (a, b, and c) and lower panels (g, h, and i), respectively. The light microscopic views are shown in d, e, f, j, k, and l.